OUTCROP-BASED SEQUENCE STRATIGRAPHY AND RESERVOIR CHARACTERIZATION OF AN UPPER MISSISSIPPIAN MIXED CARBONATE-SILICICLASTIC RAMP, MAYES COUNTY, OKLAHOMA

By

SCOTT ANDREW SHELLEY

Bachelor of Science in Geology

Oklahoma State University

Stillwater, OK

2014

Submitted to the Faculty of the
Graduate College of the
Oklahoma State University
in partial fulfillment of
the requirements for
the Degree of
MASTER OF SCIENCE
December, 2016

OUTCROP-BASED SEQUENCE STRATIGRAPHY AND RESERVOIR CHARACTERIZATION OF AN UPPER MISSISSIPPIAN MIXED CARBONATE-SILICICLASTIC RAMP, MAYES COUNTY, OKLAHOMA

Thesis Approved:

Dr. G. Michael Grammer

Thesis Adviser

Dr. James Puckette

Dr. Matthew Pranter

ACKNOWLEDGEMENTS

I'd like to start by thanking Dr. Michael Grammer. Not only for his guidance while writing this thesis, but for the lofty expectations that he holds his students to. I have learned (and retained) more useful information in the last two years than I did in four years of undergraduate work, not only because of his great advice and teaching, but because I was terrified to look stupid in front of him (not that that stopped me from doing it anyway). One day he will laugh at my jokes…one day.

I'd like to thank my committee member Dr. Jim Puckette. He taught my very first geology course at Oklahoma State, and his personality was all the confirmation I needed to know that I was in the right major and profession. He has been a great teacher and friend, and should be considered reigning Hide-and-Go-Seek champion of Oklahoma State University. I'd also like to thank my committee member Dr. Matthew Pranter. He has been most helpful on this project, providing his expertise in reservoir modeling while also helping us to work out some of the larger kinks in the drone workflow.

Big thanks to the Carbonate Clan: Miranda Childress, Buddy Price, Taylor Thompson, Beth Vanden Berg, Ashley Dupont, Yulun Wang, Ibukun Bodemoleye, Ahmed El Belasy, C.J. Appleseth, Lara Jaeckel, Elizabeth Elium, and our undergraduate assistant Skyler St. John. You guys and gals kept me sane after what feels like decades of doing research in a basement, and have been invaluable in our discussions and friendships.

I'd like to thank Josh Lambert from the Bureau of Economic Geology for his help getting started with the drone modeling. It was extremely generous of him to donate his time and help to me, and I hope to pass it forward to other students.

I, of course, need to thank my family. My parents, Don and Sandy, and my sister, Sarah, have been very patient with me over the last two years, as my visits home become more and more infrequent. They have always pushed me and supported me, even when I did something ridiculous or ill-advised.

Lastly, I must thank my fiancé, Shelby, for somehow managing to not run away by now. She has been my rock (Ha! Get it?) for the last four years, and I will continue to depend on her to calm me down and keep me moving for the rest of my life.

Name: Scott Andrew Shelley

Date of Degree: December, 2016

Title of Study: OUTCROP-BASED SEQUENCE STRATIGRAPHY AND RESERVOIR CHARACTERIZATION OF AN UPPER MISSISSIPPIAN MIXED CARBONATE-SILICICLASTIC RAMP, MAYES COUNTY, OKLAHOMA

Major Field: Geology

Abstract:

While Osagean and Kinderhookian strata have been closely studied using biostratigraphy, lithostratigraphy, and sequence stratigraphy, little work has been completed on the Meramecian and Chesterian strata of Oklahoma and Kansas. This study proposes a depositional model, sequence stratigraphic framework, and 3-D outcrop model for Upper Mississippian strata exposed in Mayes County, Oklahoma.

Facies shoal upwards from lowstand clay-rich wackestones and siltstones to progressively more carbonate-dominated facies, terminating in mud-lean skeletal packstones to grainstones. The sequence stratigraphic hierarchy present at the studied outcrop consists of two partial 3rd-order composite sequences (1-10 m.y.) constrained by biostratigraphy that are made up of probable 4th-order high frequency sequences (100 or 400 k.y.). Facies, sedimentary structures, and bed geometries observed in outcrop indicate deposition within the ramp crest to outer ramp portion of a distally-steepened ramp during various fluctuations in sea level.

Utilizing photogrammetry to stitch and geo-reference high-resolution aerial photos, 3-D representations of outcropping walls and pavement can be created at a sub-meter resolution, and can serve as valuable tools for the visualization of bed and facies relationships in 3-D space. Drone-based aerial and orthogonal photography can be used to capture images and create 3-D models of dangerous or otherwise inaccessible outcrop areas. These models can be directly imported as base surfaces to reservoir modeling software, where they can be integrated with petrographic and sequence stratigraphic data to model facies, porosity, and permeability relationships. Petrel-based facies and porosity models illustrate the lateral and vertical variability that exists in outcrop while providing detailed approximations of subsurface reservoir heterogeneity.

TABLE OF CONTENTS

Chapter Page

LIST OF FIGURES

Figure Page

LIST OF TABLES

Table Page

CHAPTER I

INTRODUCTION AND GEOLOGIC BACKGROUND

The "Mississippian Limestone" play is an unconventional oil and gas reservoir in the North American Mid-Continent that has historically produced large volumes of oil and gas, and has seen an increase in horizontal drilling with advances in drilling technology. The combination of shallow reservoir depths (3,000-6,000 ft/914-1829 m) and low drilling costs ($3-3.5 million) has made the "Mississippian Limestone" an appealing target for exploration. However, exploitation of the "Mississippian Limestone" has proved challenging due to inconsistent hydrocarbon production, high water-oil ratios, and short economic lives of wells (CoreLab, 2015). Production inconsistencies can likely be tied to internal heterogeneity within the "Mississippian Limestone" with respect to facies, flow units, and regional factors like depositional environment and structural features.

The “Mississippian Limestone” has become notorious for rapid vertical and lateral facies and flow unit changes within the subsurface (Costello, 2014). One way to mitigate these changes is to use a sequence stratigraphic approach to create a predictive model of the facies changes that likely result from multiple frequencies of relative sea level fluctuation. By creating a high resolution sequence stratigraphic framework of the “Mississippian Limestone”, meter-scale packages of rock that act as the control on fluid flow in the subsurface can be laterally predicted away from an outcrop or core data point (Grammer et al., 2004). This framework also allows for the creation of a detailed depositional model that can be used to place strata within a regional depositional context.

Previous work has addressed the broad scale depositional setting of the Mississippian section in the southern Mid-Continent, as well as more localized outcrop studies focused on macro-scale variations in lithology and biostratigraphic age constraints (Mazzullo et al. (2009), Mazzullo et al. (2013), Boardman et al. (2013), Price (2014), Leblanc (2014), Childress (2015)). Only within the last 2 years have there been studies focused on the relationship between high frequency relative sea level fluctuation and the fine-scale lateral and vertical heterogeneity seen in Mississippian outcrops and subsurface cores. Studies by Price (2014), Childress (2015) and Childress and Grammer (2016) have focused on outcrops within the tri-state area of Oklahoma, Arkansas, and Missouri, where Kinderhookian and Osagean strata are exposed, and have provided a more accurate representation of the dynamic nature of Mid-Continent Mississippian deposition. These studies, along with the subsurface core study by Leblanc

(2014) showed conclusive evidence that a hierarchy of cyclicity does exist within the Kinderhookian and Osagean strata of the Mississippian. However, very little work has been completed on the Meramecian and Chesterian strata of the Upper Mississippian, which are exposed at the Pryor Quarry near Pryor Creek, Oklahoma. By creating a detailed depositional model and placing the lithofacies variations observed at the outcrop within a sequence stratigraphic framework, 3-D geostatistical models can be created that will maximize the prediction of the lateral continuity of facies and flow units within the Upper Mississippian section.

Hypothesis and Fundamental Questions

The overarching hypothesis of this study is that a sequence stratigraphic hierarchy consisting of repeated and predictable sequences and cycles exists within the Meramecian and Chesterian strata of the "Mississippian Limestone," and provides a direct control on lateral and vertical facies and flow unit heterogeneity within the strata.

The fundamental questions posed by this research concern Mississippian deposits of Meramecian and Chesterian age in Mayes County, Oklahoma, and are as follows:

1. Does a stratigraphic hierarchy of depositional sequences and cycles exist within the Upper Mississippian strata?
2. Can minor changes in depositional facies be attributed to high-frequency relative sea level fluctuations?
3. What characteristics are most representative of reservoir and non-reservoir facies in the Pryor Quarry outcrops?

4. Can outcrop-based data and 3-D reservoir models be used to constrain subsurface analog facies and porosity models with more accurate variograms and range values?

Geologic Background

During the Mississippian Epoch (roughly 320-360 Ma), a large portion of the southern United States was submerged beneath a shallow, warm, sheltered sea (Figure 1), over which a temperate to subtropical climate persisted (Curtis and Schamplin, 1959). The Mississippian was a transitional period from Devonian greenhouse conditions to the late Pennsylvanian to Permian icehouse period (Buggisch et al, 2008).

The Lower "Mississippian Limestone" of the Mid-Continent is interpreted to have been deposited on a homoclinal ramp that evolved into a distally-steepened ramp later in the Mississippian via a series of prograding clinoforms (Boardman et al., 2010; Childress and Grammer, 2015). The distally-steepened ramp formed the southern margin of the Burlington Shelf, a shallow carbonate platform that spanned portions of Oklahoma, Kansas, Missouri, Arkansas, and Nebraska. The Burlington Shelf was bounded to the north and west by the Transcontinental Arch, to the east by the Ozark Uplift, and to the south by the Arkoma and Anadarko Basins (Lane and De Keyser, 1980.) Sediment deposited on the Burlington Shelf consisted of a mixed siliciclastic-carbonate lithology and had a depositional strike that ran roughly east-west (Mazzullo et al., 2009).

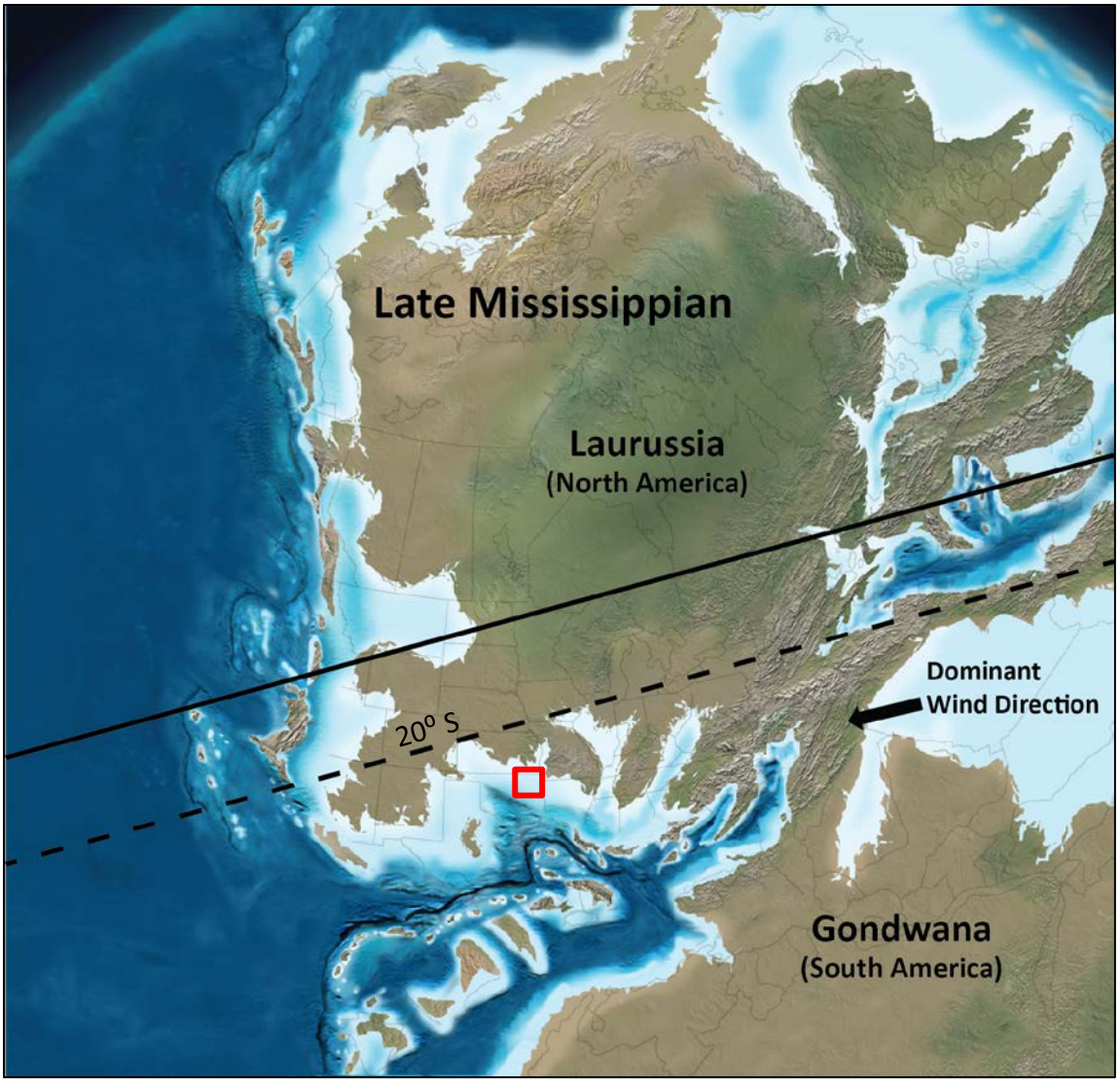

Figure 1: Late Mississippian (325 Ma) paleogeography. The study area, outlined in red, was located 25-30° south of the paleoequator. Shallow water depths are represented by light blue colors, deeper depths by darker blues. Exposed land is shown in brown and green. During this time, the study area was characterized by shallow marine conditions, was bounded to the south by deeper water, and to the east by the Ozark Uplift. The dominant wind direction is interpreted to have come from the present-day northeast, which may have had a significant impact on platform growth and geometry. Modified from Blakey (2013).

The Ozark Uplift formed sometime during the Paleozoic, and is believed to have been a paleogeographic high during Mississippian deposition (Huffman, 1958; Simms et al., 1995). Reactivation of the uplift occurred in the Pennsylvanian, creating a series of folds and faults. The uplift may have been reactivated a second time in the Late Tertiary-Early Quaternary (Simms et al., 1995). The Ozark Uplift could have served as a regional source of siliciclastics for the mixed-lithology Mississippian depositional system (Huffman, 1958).Locally, the study area is bounded by the Ozark Uplift to the east, the Nemaha Uplift to the west, and the Arkoma Basin to the south (Figure 3).

Ross and Ross (1988) identified 14-17 third-order sequences within the Mississippian, ranging from 1-3 million years in duration. Haq and Schutter (2008) identified 21 third-order sequences (Figure 4) over the same time period, also noting anomalously long sequences (1-6 million years) in the Tournaisian and Visean stages. Given that the Mississippian was a period of transitional climate, from the greenhouse conditions of the Devonian to the icehouse conditions of the Pennsylvanian, eustatic sea level fluctuations likely would have ranged between 10-100m (Read, 1995). During the Meramecian and Chesterian stages of the Upper Mississippian, sea level fluctuations likely ranged between 50-100m, as icehouse conditions became more dominant.

Figure 2: Structural features of Oklahoma. The study area is located in Mayes County, on the flanks of the Ozark Uplift, which acted as a paleogeographic high in Mississippian time (Simms et al., 1995). Modified from Northcutt and Campbell, 1996.

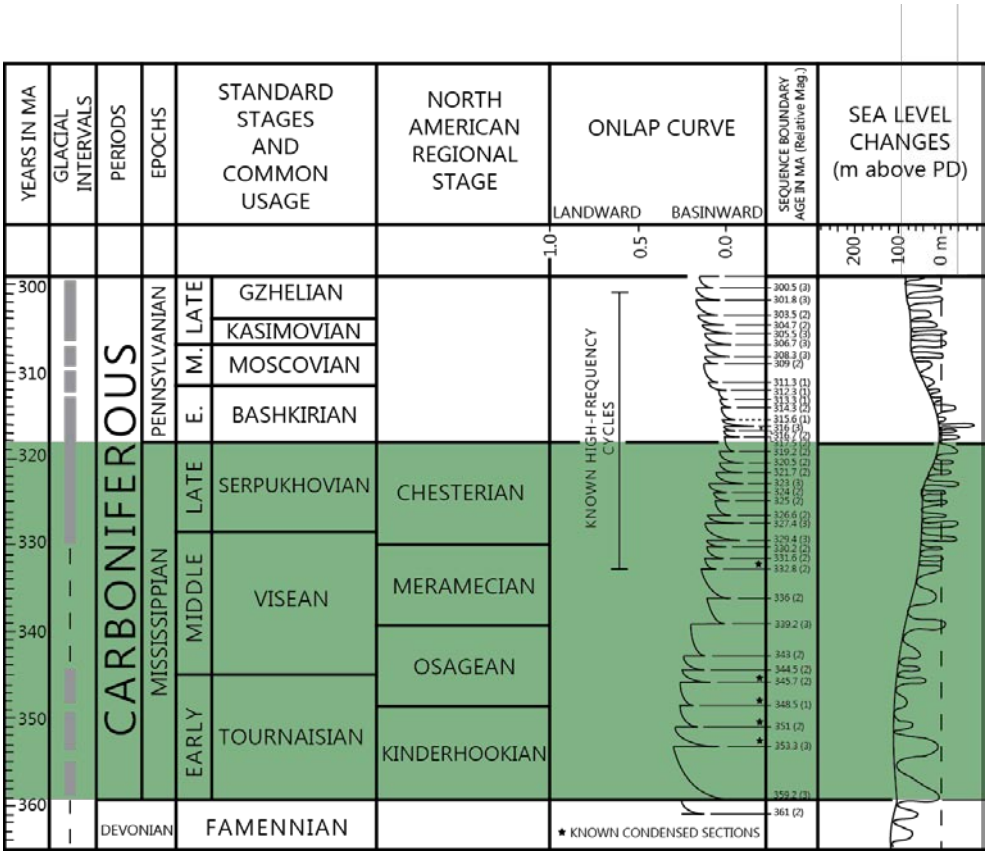

Figure 3: Diagram displaying global sea level and onlap curve for the Carboniferous Period. The Mississippian Epoch is highlighted in green. 21 third-order sequences were identified within the Mississippian. Modified from Haq and Schutter, 2008.

CHAPTER II

OUTCROP-BASED SEQUENCE STRATIGRAPHY AND RESERVOIR CHARACTERIZATION OF AN UPPER MISSISSIPPIAN MIXED CARBONATE-SILICICLASTIC RAMP, NORTHEASTERN OKLAHOMA

Introduction

Meter-scale vertical and lateral heterogeneity within carbonates has provided a challenge to academic and industry geologists for decades who attempt to characterize these complex depositional systems. Mississippian reservoirs of the North American Mid-Continent provide another example of complex facies and flow unit relationships within carbonate strata, while also offering the opportunity to study their association in the context of a mixed carbonate-siliciclastic system. Approaching reservoir characterization from an integrated perspective can help predict these relationships while also identifying controls on larger-scale depositional geometries and environments.

The aim of this study is to apply an outcrop-based approach, integrating stratigraphy, sedimentology, and modeling to evaluate Upper Mississippian reservoirs of the North American Mid-Continent, which have displayed significant heterogeneities at both reservoir and basin scales. This study demonstrates a modern workflow designed to translate data from outcrop to the subsurface via 3-D modeling of facies and porosity, while also incorporating gross depositional environments and sequence stratigraphic relationships for easier correlation and comparison to time-equivalent strata within subsurface reservoirs.

Outcrop Analogs

Outcrop-derived models are commonly used as analogs for modeling the distribution of reservoirs in the subsurface (Lucia et al., 1992; Kerans et al., 1994; Eisenberg et al., 1994; Grammer et al., 1996; Kerans and Tinker 1997; Pranter et al., 2005; Janson et al., 2007; Amour et al., 2013). Outcrop analogs provide 2-D and/or 3-D views of facies and petrophysical relationships while also offering the opportunity to collect detailed information on diagenetic events that may be controlling factors for reservoir development. While outcrop analogs may be affected by depositional and diagenetic factors not present in their subsurface equivalents, understanding the lateral and vertical relationships within outcrops that are temporally equivalent to subsurface reservoirs provides valuable data towards predicting recoveries that are often controlled by meter-scale facies and petrophysical heterogeneity. By studying and

modeling this small-scale variability in outcrop, reservoir quality, geometry, and communication of subsurface reservoirs can be more accurately predicted.

Outcrop Description

This study utilizes three outcrop walls within a quarry near Pryor Creek, Oklahoma (Figure 4). Each wall ranges from 110-225 m (365-700 ft) in length and 20-25 m (65-85 ft) in height. The Meramecian and Chesterian-aged Moorefield Formation makes up the lower portion of the outcrop, and is overlain by the Chesterian-aged Hindsville Formation (Huffman, 1958). The east (Wall 3) and west (Wall 2) walls depict a dip-oriented depositional profile, while the southern wall (Wall 1) shows a strike-oriented profile. Blasting conducted in the last decade produced vertical outcrop faces characterized by dense fracturing and little to no weathering profile, providing obstacles to sample collection and bedding delineation. Inability to safely rappel or scale outcrop faces due to fracture-based instability necessitated the use of high resolution ground-based and aerial photography in tandem with hand sample collection to trace bedding and facies continuity across each wall. The area between these outcrops covers roughly 25 ac^2 (100,000 m^2), providing the opportunity to study facies and petrophysical relationships across three 2-D othorgonal sections at a scale that is intermediary between the average well spacing of 40 ac and the meter-scale heterogeneity that typically characterizes and complicates carbonate reservoirs (Kerans, 1988; Eisenberg, 1994; Lucia et al., 2003).

Figure 4: Left: Map of Oklahoma counties. The Pryor Quarry outcrops are shown by the red star. The blue star shows the location of the Shaffer 1-23 core. Right: The Pryor Quarry outcrops consist of an E-W running wall (Wall 1) and two N-S walls (Walls 2 and 3). Satellite image modified from Google Earth (2016).

Moorefield Formation

The stratigraphic nomenclature used in this study is derived from Huffman (1958) and Mazzullo et al. (2013) (Figure 5). The Moorefield Formation makes up roughly the lower 50 ft (15.2 m) of each wall. The formation was first described by Purdue et al. (1904), and is generally characterized as a mixed argillaceous and cherty limestone with intermixed siltstone and shaly beds in Oklahoma and Arkansas (Huffman, 1958). The Moorefield Formation has previously been interpreted as a lowstand wedge deposited on a carbonate ramp (Handford, 1986). At the study area, the Moorefield Formation is made up of burrowed mudstones and bedded cherts overlain by mixed clay-rich siltstones to calcareous siltstones. Recent conodont biostratigraphic work by Godwin (2010) has shown that the Moorefield may transgress the Meramecian Chesterian series time boundary, representing conformable deposition within both series.

Hindsville Formation

The Hindsville Formation makes up the upper 15-30 ft (4.6-9.2 m) of each wall. The Hindsville Formation was first described by Purdue and Miser (1916) as an often fossiliferous limestone interbedded with shale (Huffman, 1958). The Hindsville Formation at the Pryor Quarry outcrops is characterized by skeletal wackestones to grainstones interbedded with soft, thinly bedded burrowed mudstones and silty peloidal packstones. Centimeter-scale trough cross-bedding localized within oolitic and skeletal grainstone beds is indicative of deposition under high energy conditions. The Hindsville Formation is Chesterian in age (Huffman, 1958, Godwin, 2010).

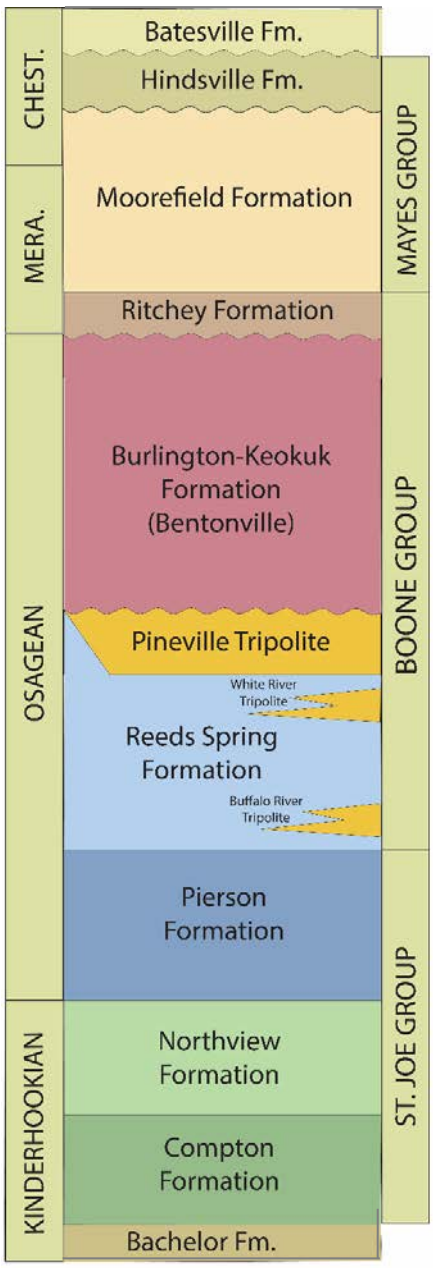

Figure 5: Stratigraphic column and nomenclature of the Mississippian section of the tri-state (OK, AR, MO) area, modified to reflect the strata present at the Pryor Quarry (modified from Mazzullo et al., 2013).

Sample Collection and Classification

Given the sheer and highly fractured nature of the Pryor Quarry outcrops, hand sample collection was limited to one measured section on the flank of each wall. The dataset gathered from the quarry included 109 hand samples, 95 thin sections, and 40 core plugs that were used to evaluate depositional facies classification, porosity, permeability, and pore characteristics (Figure 6). Allochem and cement percentages were visually estimated from thin sections (Figure 7), while porosity and permeability values were collected from core plugs via Weatherford Labs routine core plug analysis and porosimeter and permeameter measurements completed in the laboratory at Oklahoma State University. Transects were supplemented with high-resolution bedding tracing via Gigapan photos and drone-based photogrammetric images.

Wall 1 Sample Locations

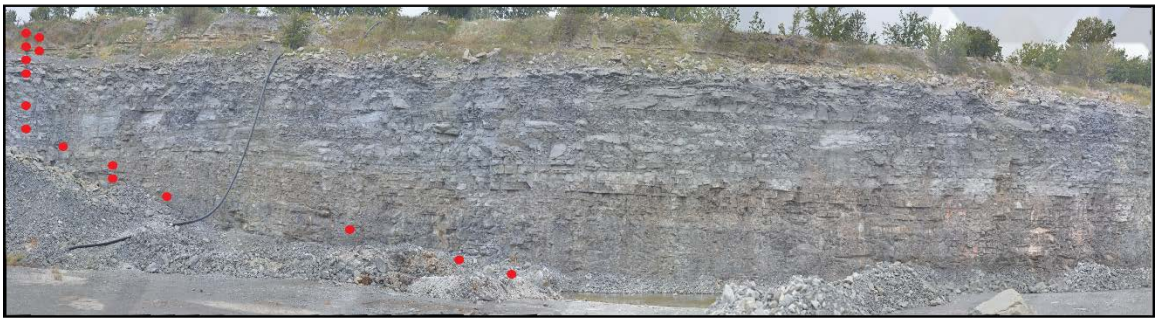

Wall 2 Sample Locations

Wall 3 Sample Locations

Figure 6: Gigapan panoramic photos of Walls 1, 2 and 3 showing the locations of collected hand samples. Thin sections and core plugs were taken from hand samples. Samples were also used for sedimentary structure recognition.

(1) Clay-Rich Quartz Siltstone: 5% ϕ

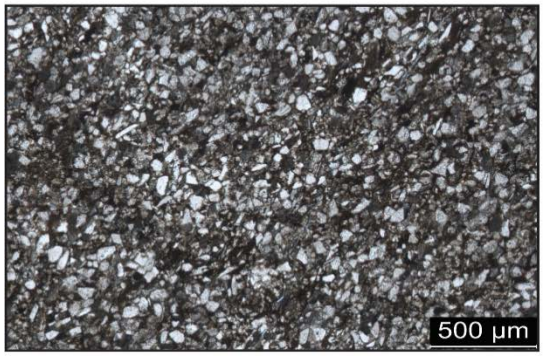

(2) Calcareous Quartz Siltstone: 5% ϕ

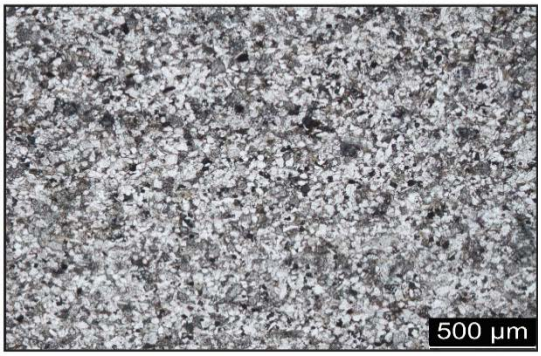

(3) Calcareous Peloidal Siltstone-Packstone: 3% ϕ

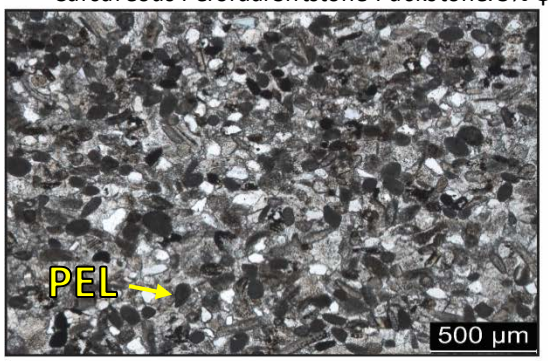

(4) Burrowed Mudstone-Wackestone: 2% ϕ

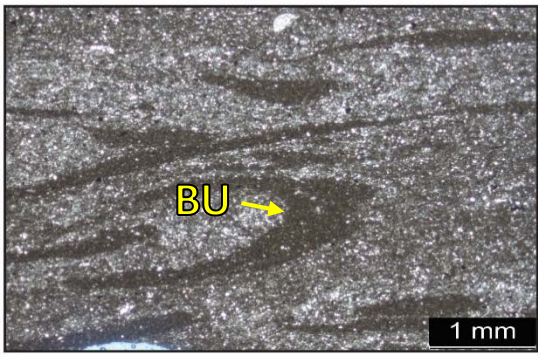

(5) Skeletal Wackestone: 2% ϕ

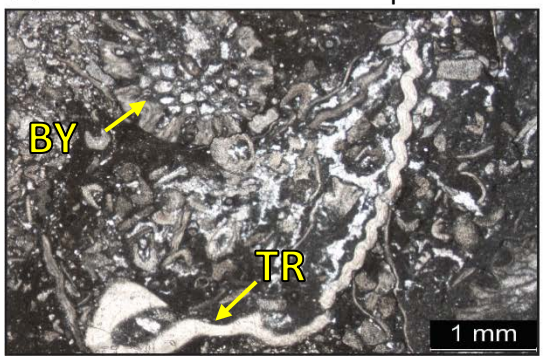

(6) Skeletal Packstone-Grainstone: 1% ϕ

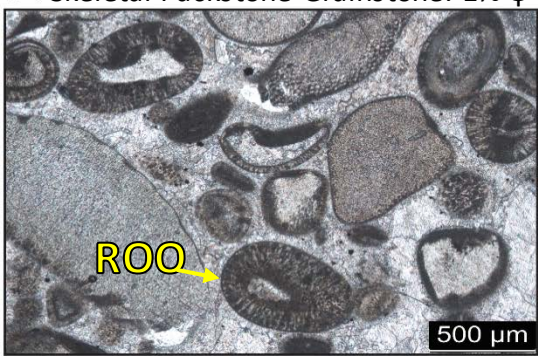

Figure 7: Thin section photomicrographs of the interpreted facies. (1) Clay-Rich Quartz Siltstone – angular quartz silt to very fine sand in a clay matrix with scattered peloids, authigenic muscovite, and pyrite. (2) Calcareous Quartz Siltstone – angular quartz silt and scattered peloids cemented with calcite and silica. (3) Calcareous Peloidal Siltstone-Packstone – Very fine to fine sand-sized peloids (PEL) and angular quartz with admixed skeletal fragments (brachiopods, crinoids, bryozoans) in a calcite and silica cement matrix. (4) Burrowed Mudstone-Wackestone – millimeter-scale clay-filled burrows (BU) in a carbonate mud and quartz silt matrix. (5) Skeletal Wackestone – normal marine skeletal fragments (brachiopods, bryozoans (BY), crinoids, trilobites (TR), echinoderms) within a carbonate mud and calcite cement matrix. (6) Skeletal Packstone-Grainstone – radial ooids (ROO) cemented with blocky calcite. Crinoid and bryozoan fragments form the nuclei for the ooids.

Depositional Facies

Facies 1 – Clay-Rich Quartz Siltstone

Facies 1 is a thinly bedded clay- and calcite-cemented siltstone to very fine-grained sandstone. Constituents include 40% very fine sand- to coarse silt-sized angular quartz grains, 35% clay cement, 5-10% calcite cement, 5-10% peloids, 5% plagioclase, <1% pyrite, and scattered brachiopod fragments that most often occur in transgressive lags.

This facies is interpreted to have been initially deposited during lowstand, and subsequently reworked into the outer ramp or offshore setting during transgression. Bedding ranges from thin and fissile to massive. Lack of recognizable cross-bedding, bioturbation, or abundant skeletal content indicates low energy deposition in waters that were not conducive to normal marine fauna. Angular, moderately sorted quartz sand and silt reflects initial deposition via eolian processes before reworking, while the presence of brachiopod lag beds (0.1-0.75 m in thickness) and rare carbonate intraclasts may represent incorporation of underlying carbonate-rich sediments during particularly rapid transgression (Handford and Loucks, 1993). Fractures and intergranular pores contribute to an average porosity of 5% and permeability of .003 mD.

Facies 2 – Calcareous Quartz Siltstone

Facies 2 is a calcite- and silica-cemented quartz siltstone. Silt-sized, angular, and likely eolian-derived quartz composes 30-50% of Facies 2, along with 40-60% calcite and silica cement, 1-5% peloids, <1% authigenic muscovite, and <1% pyrite. Facies 2 is

distinguished from Facies 1 by a smaller proportion or lack of clay minerals and a corresponding increase in calcite cement.

Significant post-depositional cementation is present in the form of porosity-occluding calcite and silica cement, the latter commonly occurring as quartz overgrowths. Similarly to Facies 1, Facies 2 lacks recognizable sedimentary structures, skeletal content, and bioturbation, indicating deposition in the mid to outer ramp or lower shoreface to offshore environment in low energy, restricted waters. The relative lack of clays may indicate continued transgression, as increasing water circulation results in higher dispersion of clays. Fracture and intergranular pores contribute to an average porosity of 5% and permeability of .002 mD.

Facies 3 – Calcareous Peloidal Siltstone-Packstone

The calcareous peloidal siltstone-packstone facies is characterized by tan-colored, massive, meter-scale bedding with scattered oxidized pyrite. Quartz content (likely eolian) varies from 20-70%, and is typically inversely proportional to peloid content, which can range from 5-30%. Facies 3 contains abundant calcite and silica cements as well as common benthic foraminifera tests.

Multiple sedimentary features described from the Pryor Creek outcrops are unique to Facies 3. Dense *Palaeophycus* and *Skolithos* burrows and centimeter-scale symmetrical ripples present at the top of the Moorefield Formation indicate shallow marine deposition under high energy conditions (Dott and Bourgeouis, 1982; Gaillard and Racheboeuf, 2006). Localized millimeter-scale mud layers indicate occasional storm influence. The dip-oriented Wall 3 exhibits horizontal beds that grade laterally into

meter-scale imbricated to shingled bed geometries. These shingled beds display a progradational geometry, partially filling a hemispherical break in bedding that may represent a storm channel cut. The cut is further filled by thinly bedded, horizontal siltstones. Facies 3 was deposited in the lower shoreface to ramp crest environment. The meter-scale shingled beds at the top of the Moorefield Formation may have been deposited as a shallow subtidal bar cut by a storm channel (Figure 8). Horizontal beds represent the main body of the bar, while shingled beds reflect current-driven progradational filling of the storm channel, similar to geometries observed in modern offshore Texas environments (McCubbin, 1981). More peloidal-rich beds of Facies 3 may represent deposition in a low-energy lagoon created by the presence of the offshore bar. Facies 3 is more heavily cemented with calcite and silica than previous facies, but still exhibits an average porosity of 3% and permeability of .0002 mD, contained within fracture and intergranular pores.

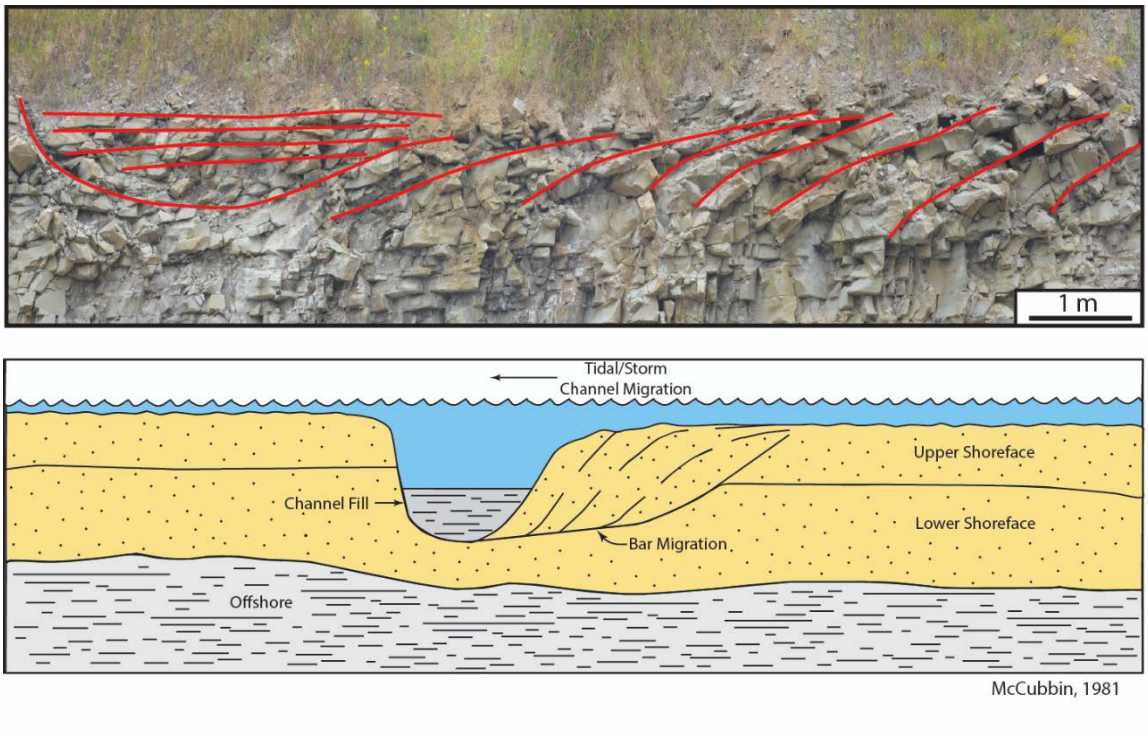

Figure 8: Offshore siliciclastic bar geometry observed within Wall 3. Meter-scale shingled beds prograde northward before being truncated by a storm channel cut. The channel cut is filled with flat-lying beds of Facies 2. Samples of Facies 3 with high peloidal content were likely deposited behind the bar system, where quiet water conditions would be ideal for peloid formation.

Facies 4 – Burrowed Mudstone-Wackestone

Facies 4 is a burrowed mudstone to wackestone with interbedded chert-rich layers. Muddy layers contain about 85% carbonate mud, 15% quartz silt, and <1% pyrite. Cherty layers range up to 50% quartz, 45-50% carbonate mud, and 1-5% pyrite. Chert content may be related to abundant sponge spicules that are observable in thin section (Facies 4 only) and are commonly partially replaced by pyrite. Blocky calcite and chert cements occur within fractures, which are common in the chert-rich layers.

Facies 4 was likely deposited in relatively deep water under low energy conditions based upon the high carbonate mud content, extensive burrowing, and spicule-dominant fauna observed in both thin section and outcrop. The presence of

sponge spicule-dominated fauna may be an indicator of restricted, deep water deposition (Goldhammer et al., 1991). Alternating mud- and chert-rich layers hint at high-order cyclicity, possibly related to spicule or mixing zone chertification (Knauth, 1979). It is unclear whether this cyclicity is due to autocyclic or allocyclic processes. Facies 4 contains no visible pores, with micro- to nano-scale pores likely contributing to its average porosity of 2%. The average permeability value of Facies 4 was below the resolution of the core analysis (<.0001 mD)

Facies 5 – Skeletal Wackestone

Facies 5 is a skeletal wackestone composed of 45% carbonate mud, 35% skeletal fragments, 10% blocky calcite cement, and 10% quartz silt. The skeletal content includes a normal marine faunal assemblage of (in order of abundance): brachiopods, crinoids, bryozoans, echinoderms, and trilobites. Facies 5 typically occurs in decimeter-scale beds without obvious sedimentary structures, but is also observed with centimeter-scale burrow fills within shale-like siltstone beds underlying grainier carbonate beds, indicating depositional conditions that were conducive to large burrowing organisms.

The observed normal marine faunal assemblage indicates normal water conditions in intermediate water depths and energy regimes. Facies 5 was likely deposited in a middle ramp environment, seaward of the ramp crest. Facies 5 exhibits moldic porosity likely related to recent subaerial exposure, with an average porosity of 2%. The average permeability value of Facies 5 was below the resolution of the core analysis (<.0001 mD)

Facies 6 – Skeletal Packstone-Grainstone

Facies 6 consists of both skeletal and non-skeletal carbonate grains within calcite cement and carbonate mud matrix. Fabrics vary from a mud-lean packstone to grainstone cemented with blocky calcite. The faunal assemblage within Facies 6 is similar to that of Facies 5, containing bryozoans, crinoids, brachiopods, benthic foraminifera, trilobites, and echinoderms, in order of abundance. Facies 6 differs from Facies 5 in that it contains well-preserved gastropods and both radial and tangential ooids. In outcrop, Facies 6 exhibits centimeter-scale bi-directional cross-bedding.

Low mud content, allochem type, and cross-bedding indicate that Facies 6 was deposited in shallow, high energy waters, likely in a skeletal shoal environment proximal relative to Facies 5 deposition. Similar to Facies 5, Facies 6 exhibits minor moldic porosity likely related to recent subaerial exposure, with an average porosity of 1%. The average permeability value of Facies 6 was below the resolution of the core analysis (<.0001 mD)

Sequence Stratigraphy

Facies were placed within an idealized vertical stacking pattern determined by their interpreted depositional environment and relationship to sea level (Figure 9). The sequence stratigraphic architecture represented in this study includes a two-fold hierarchy of depositional sequences that represent cyclical changes in sea level and corresponding changes in depositional conditions (Figure 10). Biostratigraphic data from Godwin (2010) was used to constrain the age of these outcrops down to a resolution of 4-6 million years. The Pryor Creek outcrops contain two partial to complete 3rd-order

sequences and three to four 4th-order sequences. The 3rd-order sequence at the base of the outcrop is incomplete, recording only the regressive phase of an idealized sequence. Sequence stratigraphic variability between walls is due to differences in erosion at the top of the outcrop exposures. The quarry floor was mined along an unconformity due to specific mineralogical requirements for Oklahoma state aggregate production, which provides confidence that the lowermost and uppermost sequences correlated between outcrop walls are bounded by geologically time-equivalent surfaces.

Sequence boundaries are characterized by either a significant increase in water depth from inner to mid ramp facies below the surface to outer ramp facies above or by geologically significant surfaces such as lag deposits or rip-up surfaces. The Moorefield Formation contains a high percentage of siliciclastic facies relative to the Hindsville Formation.

The transgressive phase of an idealized sequence is characterized by siliciclastic-dominated facies (1-3) as sea level rises and reworks eolian quartz silt and fine sands as well as clays deposited during lowstand. The initial transgression is often marked by rip-up of underlying carbonates or shell lags. Facies 4 represents the deepest water deposition, as carbonates begin to dominate the system. Facies 4-6 represent a typical regressive carbonate sequence, culminating in the skeletal and oolitic inner ramp shoals of Facies 6. Repeated transgressions and regressions of sea level create both vertical and lateral facies heterogeneities that often create compartmentalized reservoirs in many carbonate systems (Grammer et al., 1996).

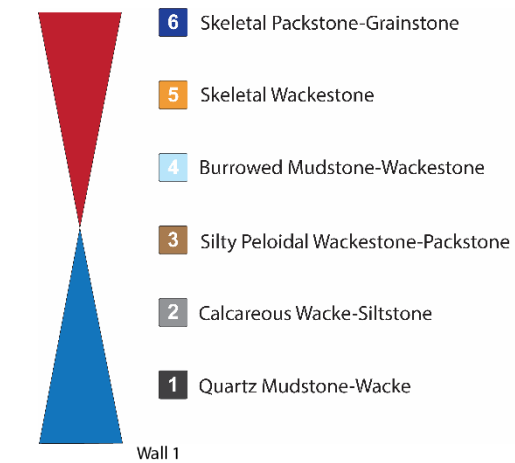

Figure 9 (top): Idealized vertical stacking pattern. Facies 1-3 are interpreted to have been deposited during sea level transgression, Facies 4-6 during regression.

Figure 10 (bottom): Sequence stratigraphic architecture of the three outcropping walls. Three 3rd-order sequences and four to five 4th-order sequences are recognizable within the outcrops. The unconformity surfaces represent the base of the Moorefield Formation and top of the Hindsville Formation.

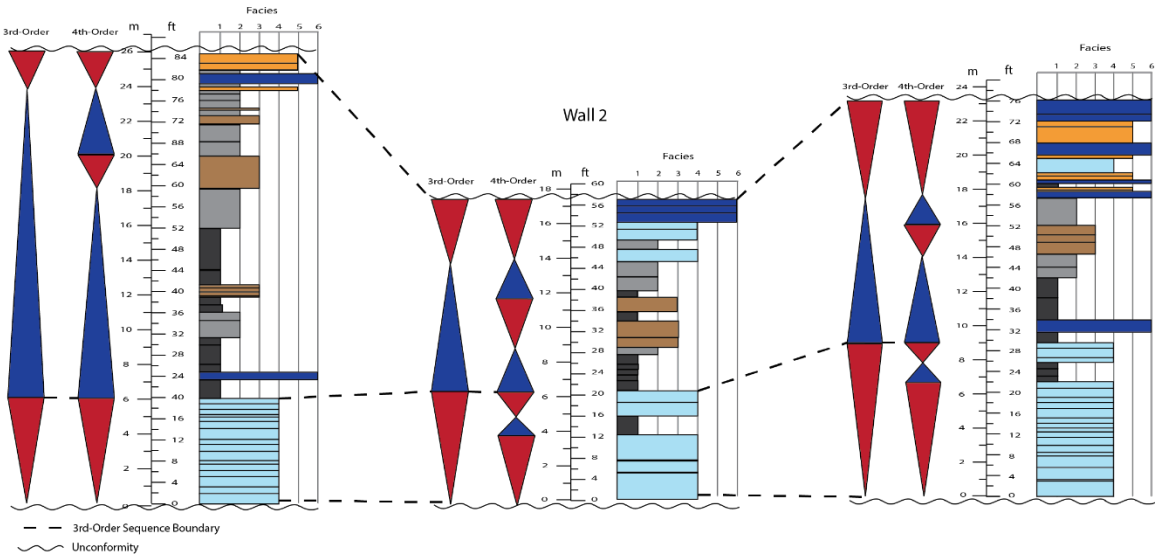

Bedding Relationships and Depositional Model

Bedding geometry and tracing of bed continuity provides a valuable tool for delineating sequence boundaries and identifying depositional environments and structural influences. A Gigapan Epic Pro was used to stitch approximately three thousand individual photos together to create gigapixel panorama images of each wall with centimeter-scale resolution (Figure 11). These photos are useful in identifying sedimentary structures and bedding boundaries on inaccessible outcrop walls such as those in the Pryor Quarry.

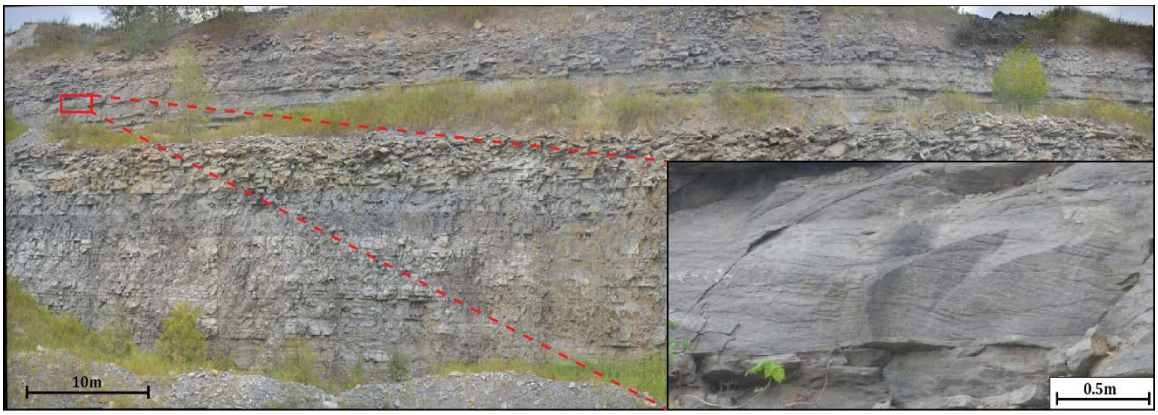

Figure 11: Panoramic GigaPan photo of Wall 3 consisting of roughly 1,000 individual photos. Inset: GigaPan resolution allows for the recognition of centimeter-scale sedimentary features such as cross-beds within an ooid and skeletal shoal.

Previous work has identified the likely depositional setting of the Mid-Continent Mississippian as a distally-steepened ramp, as evidenced by prograding clinoforms and debris flow-supported outrunner blocks (Boardman et al., 2010; Childress, 2015; Childress and Grammer, 2016). The observations made from the Pryor Quarry are consistent with this general model, however, the introduction of a source for terrestrial

eolian silt and cyclic siliciclastic-carbonate depositional sequences within the system add another layer of complexity to the sedimentologic record of the ramp system (Figure 12). Siliciclastic input into the basin likely occurred through multiple sources. The well-sorted, angular, quartz silts that are present in all facies (in various proportions) likely represent eolian processes that were active throughout the interval of deposition recorded at the Pryor Quarry. In addition to eolian quartz silts, fluvial or deltaic derived siliciclastic sediments may have contributed to the feldspar and clay content of Facies 1 and 2. Siliciclastic input into the basin likely suppressed carbonate sedimentation, creating muddier water conditions that would not be conducive to carbonate-producing organisms that rely on photosynthesis or filter feeding.

The rocks in the Pryor Quarry represents deposition ranging from the ramp crest, as indicated by the presence of the bar and shoal geometries of Facies 3 and 6, respectively, to the outer ramp, evidenced by the increased clay content and lack of normal marine fauna of Facies 1 and 2. The siliciclastic bar of Facies 3 likely formed an antecedent topographical high for Facies 6 carbonate shoal development (Figure 13). This is a significant line of evidence to support the idea that sea level forms the main control on the overall shift from siliciclastic to carbonate sedimentation.

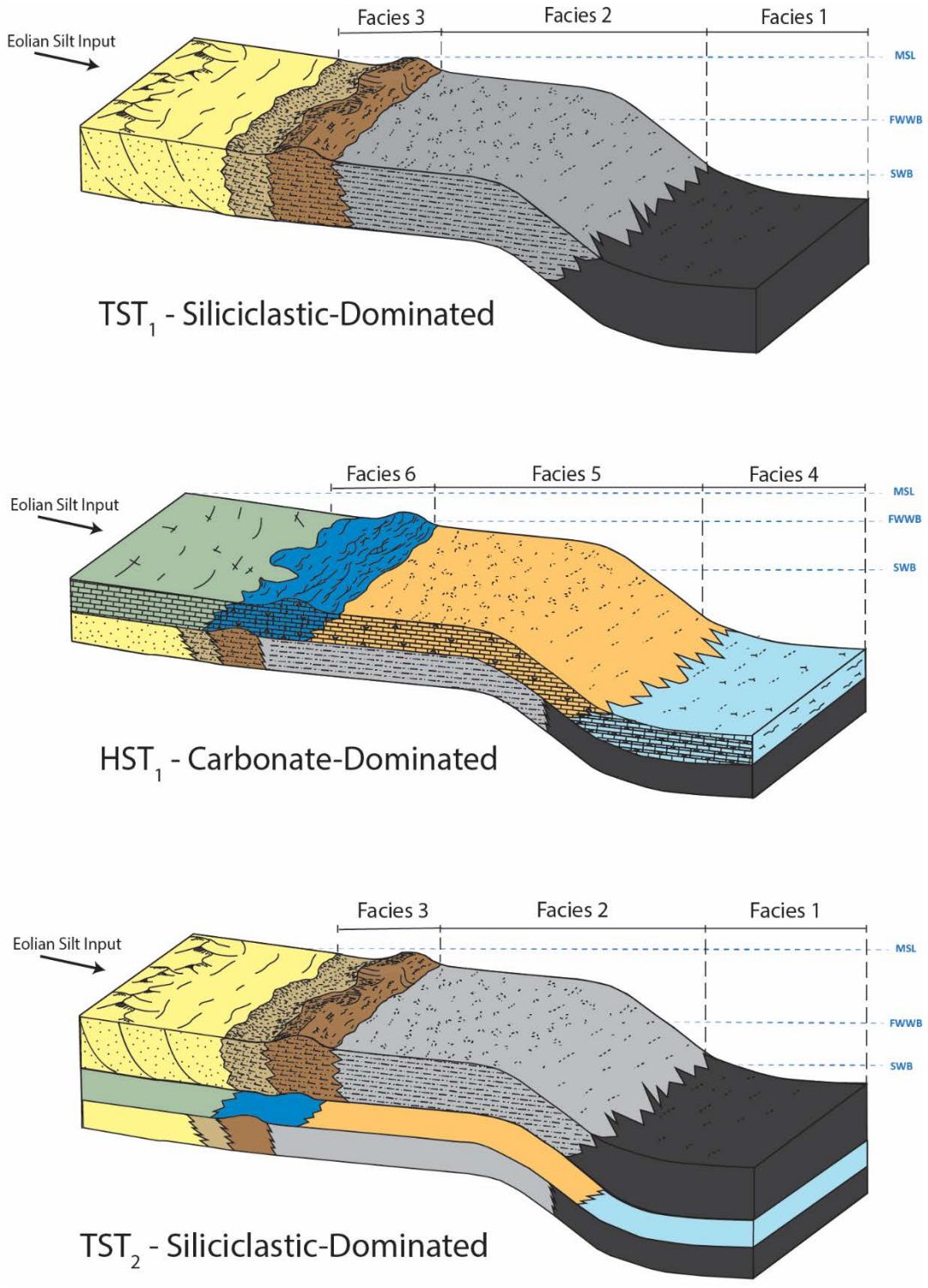

Figure 12: Block diagram showing cyclical changes in sedimentological dominance derived from relative sea level changes within the distally-steepened ramp system. Siliciclastic sedimentation becomes dominant during lowstand and transgression, while carbonate sedimentation is dominant during highstand. Repeated sea level changes serve to complicate the stratigraphic record through related lateral migration of facies.

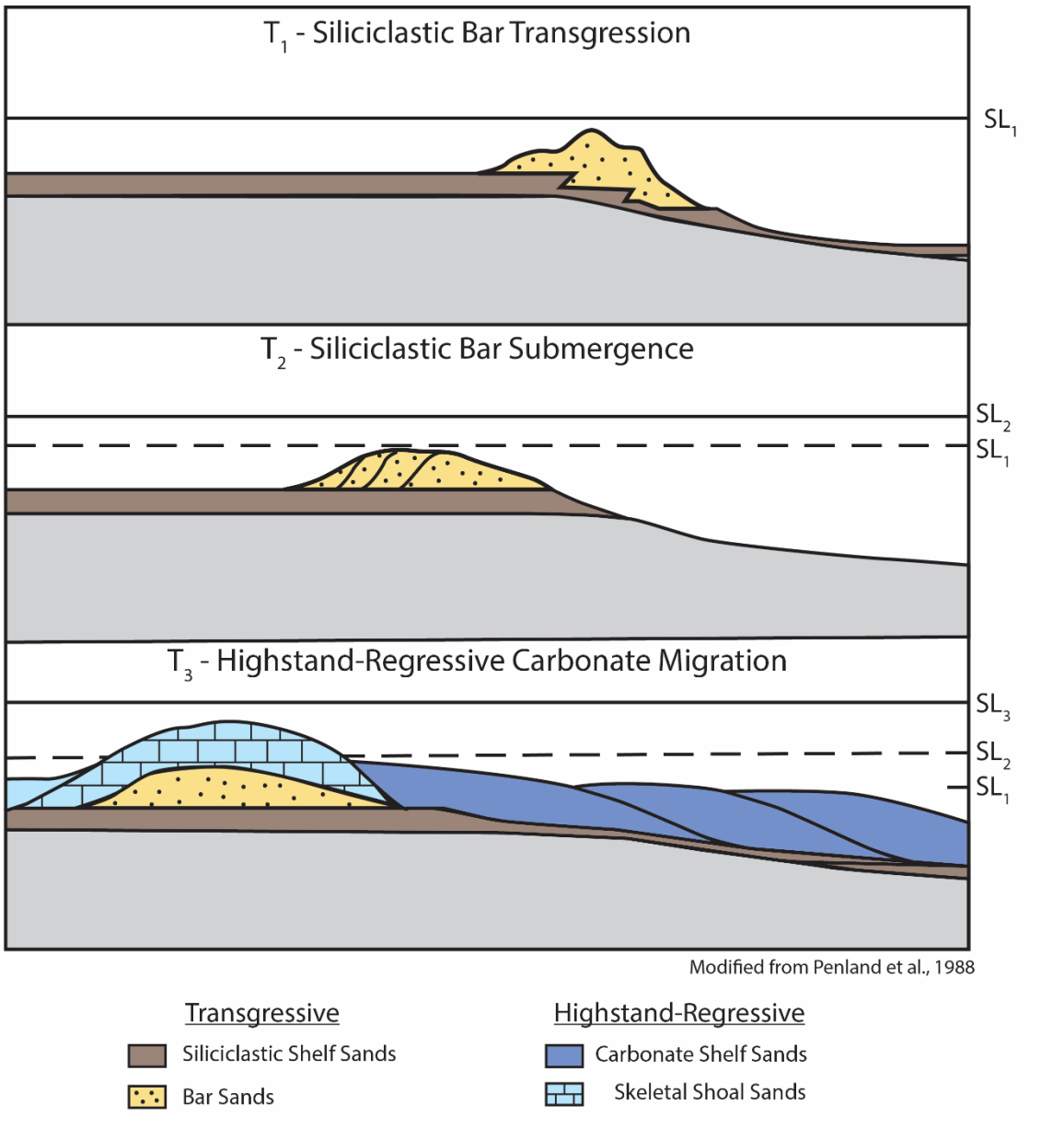

Figure 13: Evolution of bar geometries related to sea level change. The siliciclastic bar formed during lowstand is re-worked and progrades shoreward during transgression before serving as an antecedent high for highstand carbonate shoal formation.

Gamma-Ray

Recent work studying subsurface Carboniferous mixed carbonate-siliciclastic systems have identified a correlation between spectral gamma ray signatures and sequence boundaries that allow for the approximation of sequence boundaries using subsurface wireline logs (Ehrenberg and Svånå, 2000; LeBlanc and Grammer, 2014; Flinton, 2016). Positive shifts in total spectral gamma ray curves related to lithology changes and exposure surfaces at boundaries are often clearly identifiable at the 3rd- and 4th-order sequence scale. While this pattern has been fairly consistent when used in core-based studies in the Mid-Continent region, little to no correlation has been observed in outcrop exposures.

Using an Exploranium GR-320 envi-SPEC scintillometer, a vertical spectral gamma ray signature was collected along the dip-oriented Wall 3 transect (Figure 14). The spectral gamma ray signature correlates with the top of only one 4th-order sequence, located within the Hindsville, and is not an accurate representation of facies or sequence boundaries. These results, combined with those of Childress (2015) and Price (2016), suggest that gamma-ray signatures may only be useful in identifying subsurface sequence boundaries within the Mid-Continent Mississippian. The Pryor Quarry outcrops are overlain by 2-5 ft (0.6-1.5m) of clay-rich soils that often stain the outcropping faces during rainfall. While efforts were made to measure gamma ray signatures at clean surfaces, incorporation of these clays into the outcrops would create

a significant overprint on the original signatures.

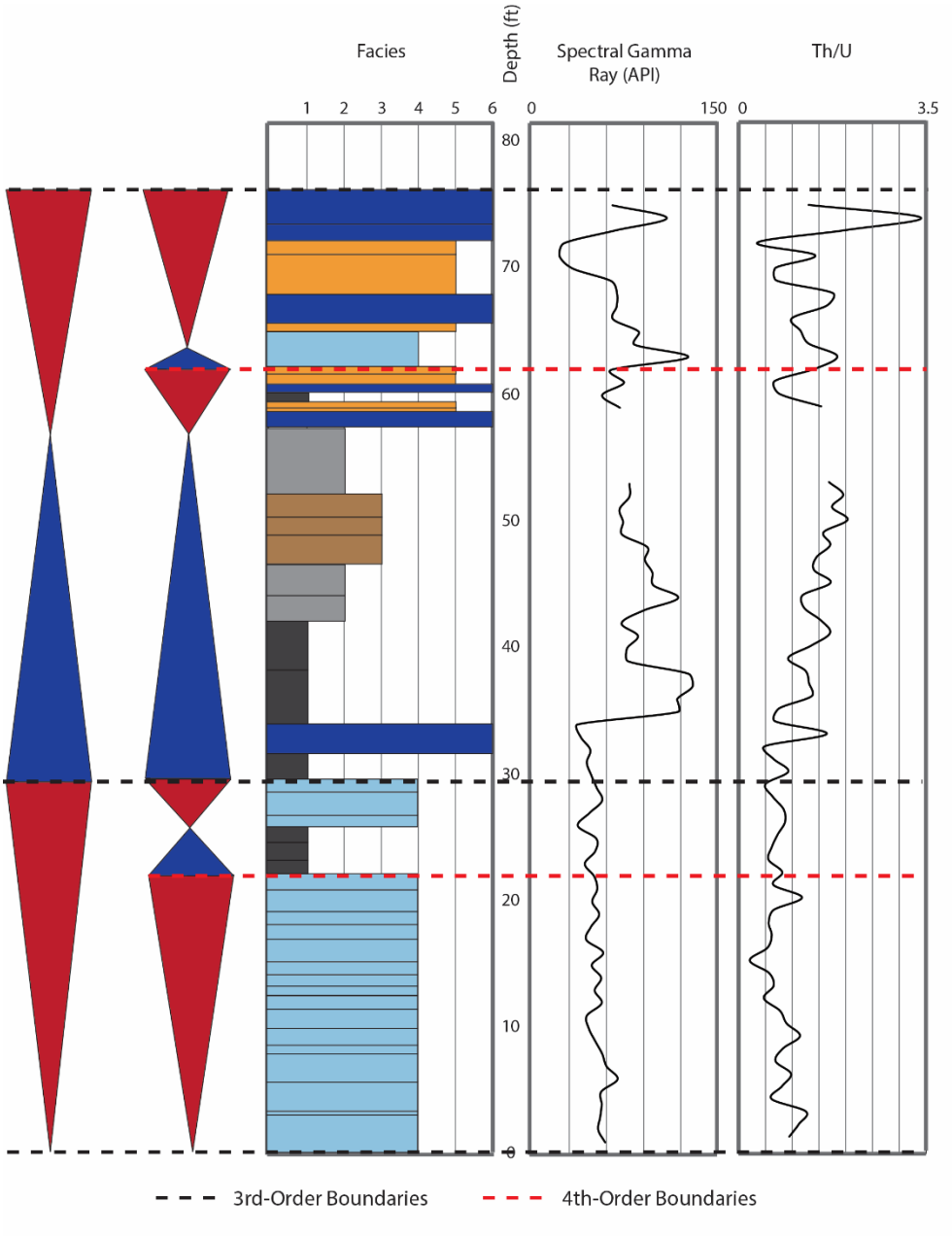

Figure 14: Vertical section of Wall 3 with spectral gamma-ray and Th/U signatures. Sequence boundaries do not correlate well to gamma-ray, likely due to outcrop diagenetic alteration. Th/U increases towards the top of the Moorefield Formation, indicating increased terrestrial input.

Reservoir and Pore Characterization

The classic carbonate ramp model suggests highest depositional energy located nearest to shoreline, barring the development of a ramp crest (Ahr, 1973; Burchette and Wright, 1992). A distally steepened ramp geometry should follow this same pattern, generally characterized by grainy, high porosity facies in proximal positions and muddier, low porosity facies in distal positions. As an example, the mixed carbonate-siliciclastic systems of the Paradox Basin (Pennsylvanian) and Leonardian deposits of the Permian Basin exhibit the highest porosity intervals within shallower water carbonate facies, while the siliciclastic facies often act as seals (Mazzullo and Reid, 1989; Grammer et al., 1996; Ruppel and Ward, 2013). Patterns of porosity development within the Pryor Quarry strata deviate significantly from this model. Shallow carbonate facies (Facies 5 and 6) within the Moorefield and Hindsville Formations have been occluded with calcite and silica cements and act as vertical seals, while deep water siliciclastic facies (Facies 1 and 2) represent the reservoir facies (Figure 15).

The dominant pore types within the siliciclastic reservoir facies are intergranular, intragranular/moldic, and fracture pores (Figure 16). All siliciclastic samples with visible porosity show signs of dissolution enhancement, likely as a result of feldspar dissolution (Figure 16-C). Despite low permeability values, pores do seem to be connected by dissolution-enhanced micro-fractures.

Porosity is inversely proportional to the percentage of calcite cement within a sample. Facies 1, the clay-rich quartz siltstone, contains the smallest calcite percentage and highest clay content of any facies, while also exhibiting the highest porosity. The

majority of clays within Facies 1 are likely depositional, though some clays may be authigenic, sourced from the dissolution of feldspar grains. Clay coatings are frequently cited as inhibitors of quartz overgrowth cements in deep sandstone reservoirs, preventing the nucleation of cements on grain faces and preserving porosity (Pittman and Lumsden, 1968; McBride, 1985; Dixon et al., 1989). Inhibition of calcite cement by clays has been less frequently documented, but likely acts through a similar process, preventing calcite nucleation on grains (Buxton and Sibley, 1981; Moraes and De Ros, 1990).

While clay minerals seem to preserve feldspar dissolution-derived porosity, they also act to severely reduce permeability (Moraes and De Ros, 1990). The primary pores are largely kept open, but pore throats and pore-connecting fractures are generally occluded, resulting in the extremely low range of permeability values recorded from the Pryor Quarry samples (.0001-.007 mD).

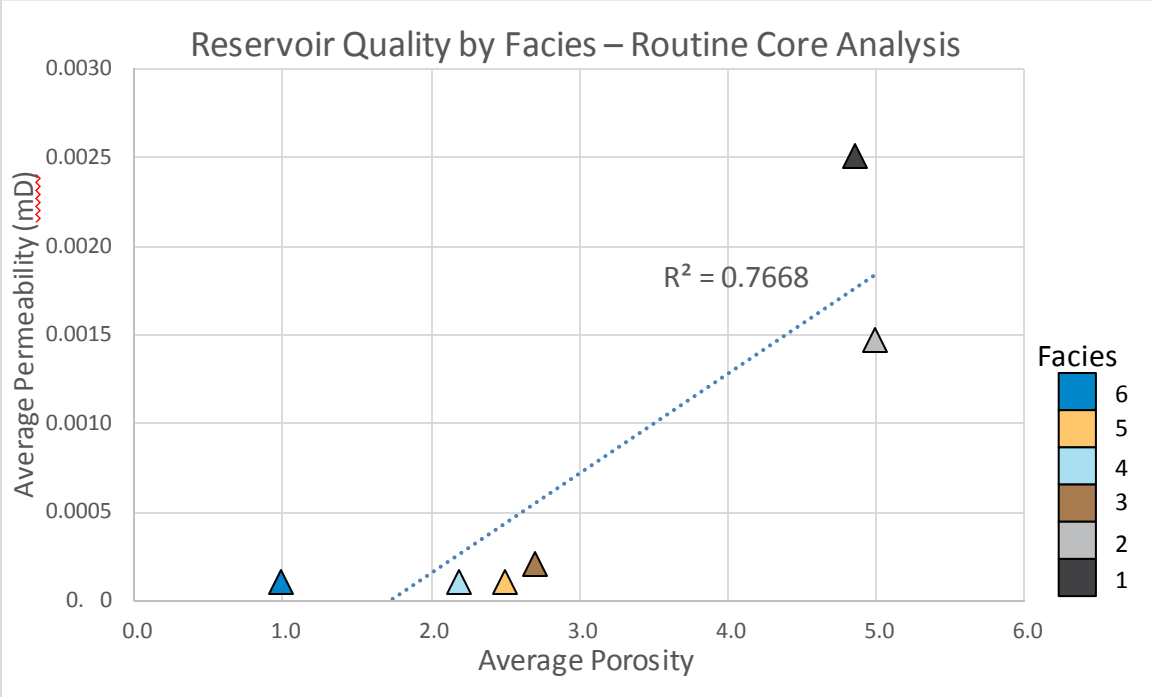

Figure 15: Cross-plot of core plug porosity and permeability. Facies 1 and 2 have the highest reservoir quality, while Facies 3-6 would likely form seals in the subsurface. Porosity is likely controlled by diagenetic calcite cement content, which may be inhibited by clay rims in Facies 1 and 2.

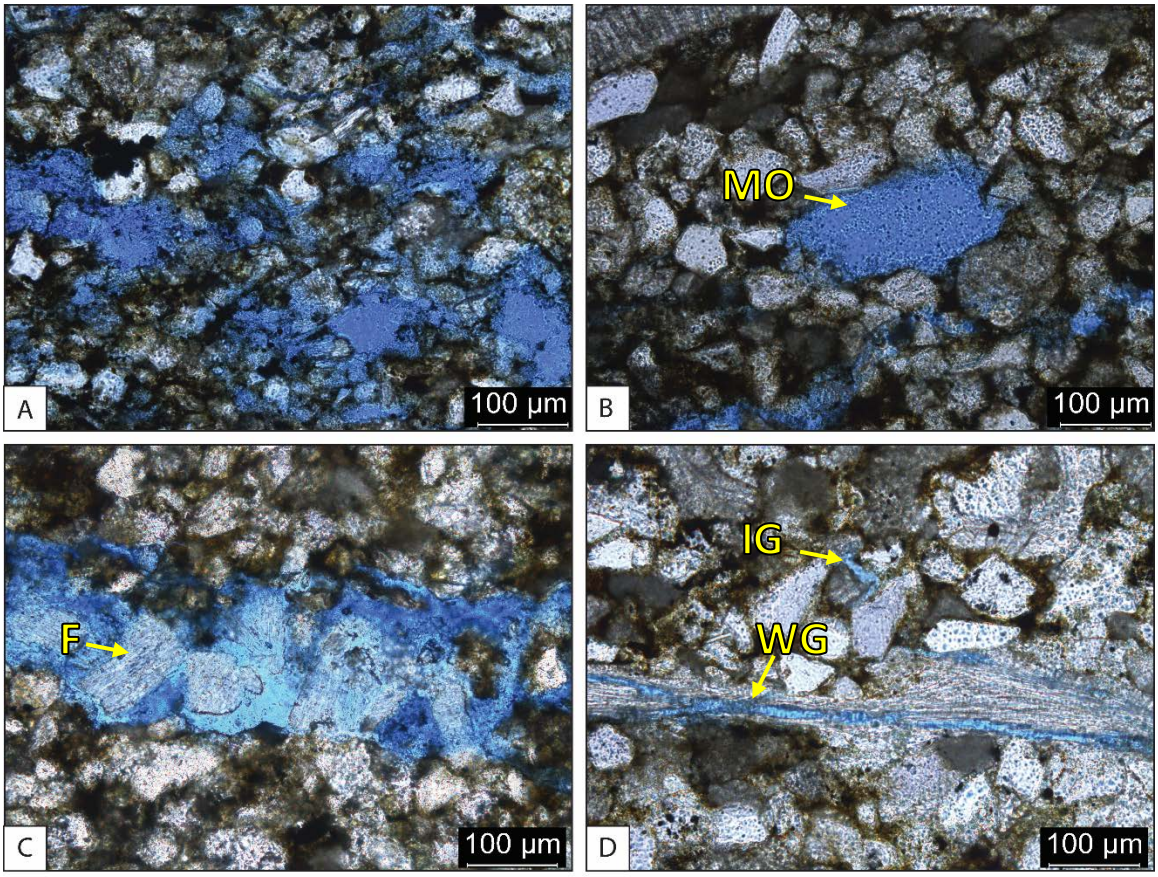

Figure 16: Thin section photomicrographs showing the primary pore types within the siliciclastic Facies 1. (A) Primary and dissolution-enhanced intergranular and moldic porosity. (B) Moldic and fracture porosity (MO). (C) Dissolution-enhanced fracture porosity. Fracture fill is composed of partially dissolved feldspar fragments (F). (D) Intergranular porosity between quartz grains (IG) and intragranular (WG) porosity within a brachiopod fragment.

SEM microscopy

Individual pores, pore networks, and pore fills were evaluated using a scanning electron microscope to better characterize the Facies 1 reservoir potential (Figure 17).

While mesopores (62.5 µm – 4 mm) were observed, the majority of the pores evaluated fall within the micropore (1-62.5 µm) to nanopore (1 nm – 1µm) range. Individual pores are typically coated and/or filled with clay material, typically montmorillonite or illite-smectite mixed-layer clay. Pore throats tend to be narrow, often clogged with clay minerals, however the pores are fairly well-connected via a network of microfractures, most often with apertures ranging from 1-3 µm. No calcite crystal growth was observed in any sample of Facies 1.

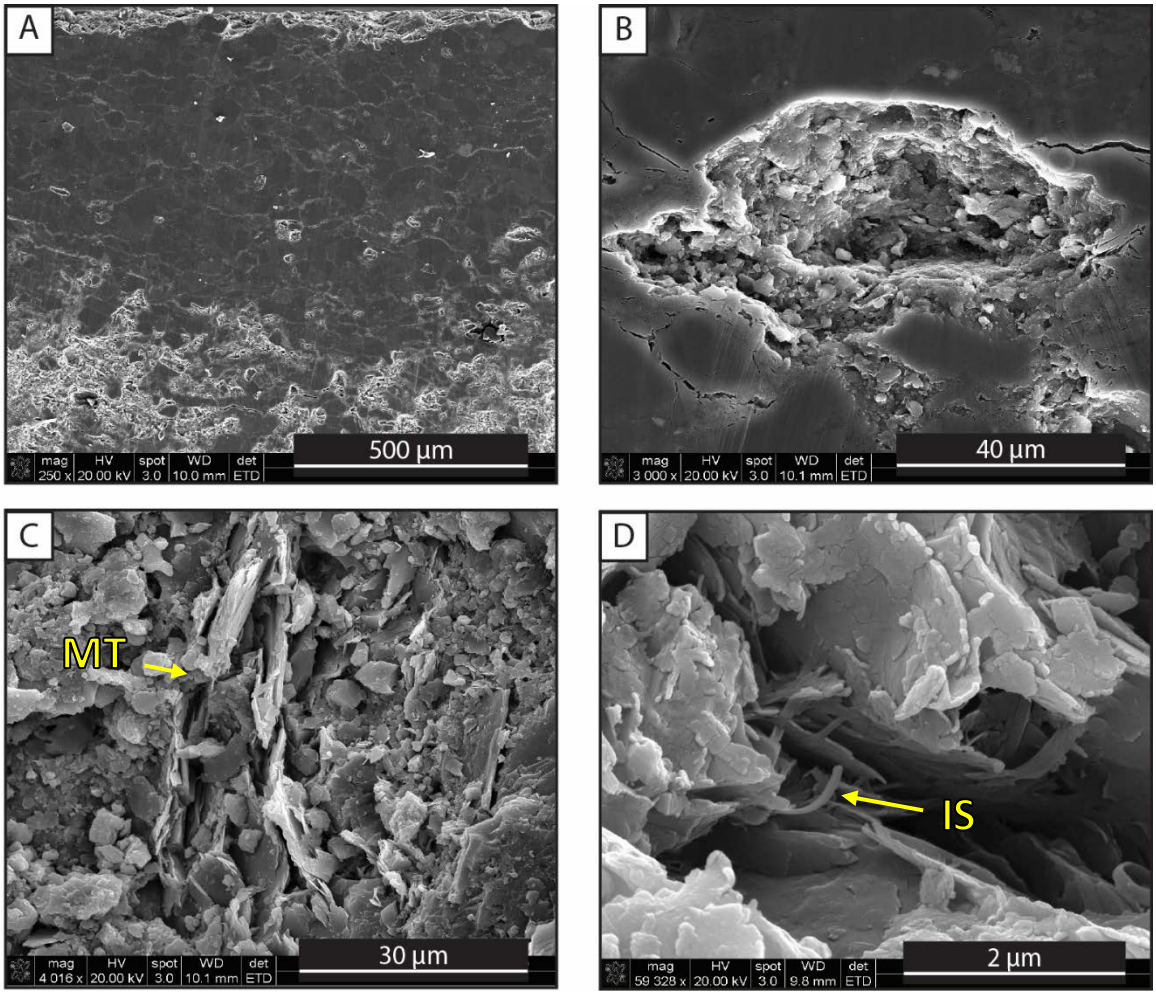

Figure 17: SEM photomicrographs of Facies 1. **A**: Ion-milled sample showing the overall pore size distribution which ranges from 1 nm – 100 µm. **B**: Clay-coated mesopore. **C**: Porosity-occluding montmorillonite (MT). **D**: Pore-lining illite-smectite mixed-layer clays (IS). Clay minerals likely act to inhibit late diagenetic calcite cementation, thus preserving porosity within Facies 1. While clays occlude larger pores and most pore throats, micro- and nanopores occur between clay layers and contribute to total porosity.

Analog Reservoir – Shaffer 1-23 Core, STACK Play

The siliciclastic facies within the Pryor Quarry serve as a lithological analog for the STACK (Sooner Trend, Anadarko (Basin), Canadian and Kingfisher (Counties)) play of Oklahoma, which consists of stacked reservoirs of the Woodford Shale and Mississippian mixed carbonate-siliciclastic sections. The STACK play is the most active play in the southern Mid-Continent with completions targeting the "Mississippi Lime" (naturalgasintel.com), targeting the thick intervals of silt-rich siliciclastics and carbonates.

To compare the Pryor Quarry Facies 1 to typical Mississippian STACK reservoir lithologies, thin section photomicrographs from the Shaffer 1-23 core were examined and compared to outcrop samples (Figure 18).The Shaffer 1-23 is located in Blaine County, OK, on the north flank of the STACK Play. Both samples contain similar constituents and matrix, as well as similar porosity values. Lithologies similar to Facies 2 and 3 also occur within the Shaffer 1-23, but, similar to what is observed in outcrop, greater calcite cementation leads to lower porosity content. Higher depositional clay content may inhibit calcite cementation in the Facies 1 reservoir type, preserving void space. Pryor Quarry and Shaffer 1-23 clay minerals seem to have similar morphologies, resulting in the development of micro- and nanopores between pore coating clays. Shaffer pores exhibit pore throats clogged by clays, but seem to be characterized by greater overall connectivity than similar pore systems from Pryor Quarry samples. The

Shaffer 1-23 lies in a distal position relative to the Pryor Quarry, and does not contain clean carbonate facies.

By studying the facies and reservoir relationships at the Pryor Quarry outcrops, a first-order approximation of STACK reservoir relationships can be created to act as a tool in reservoir prediction.

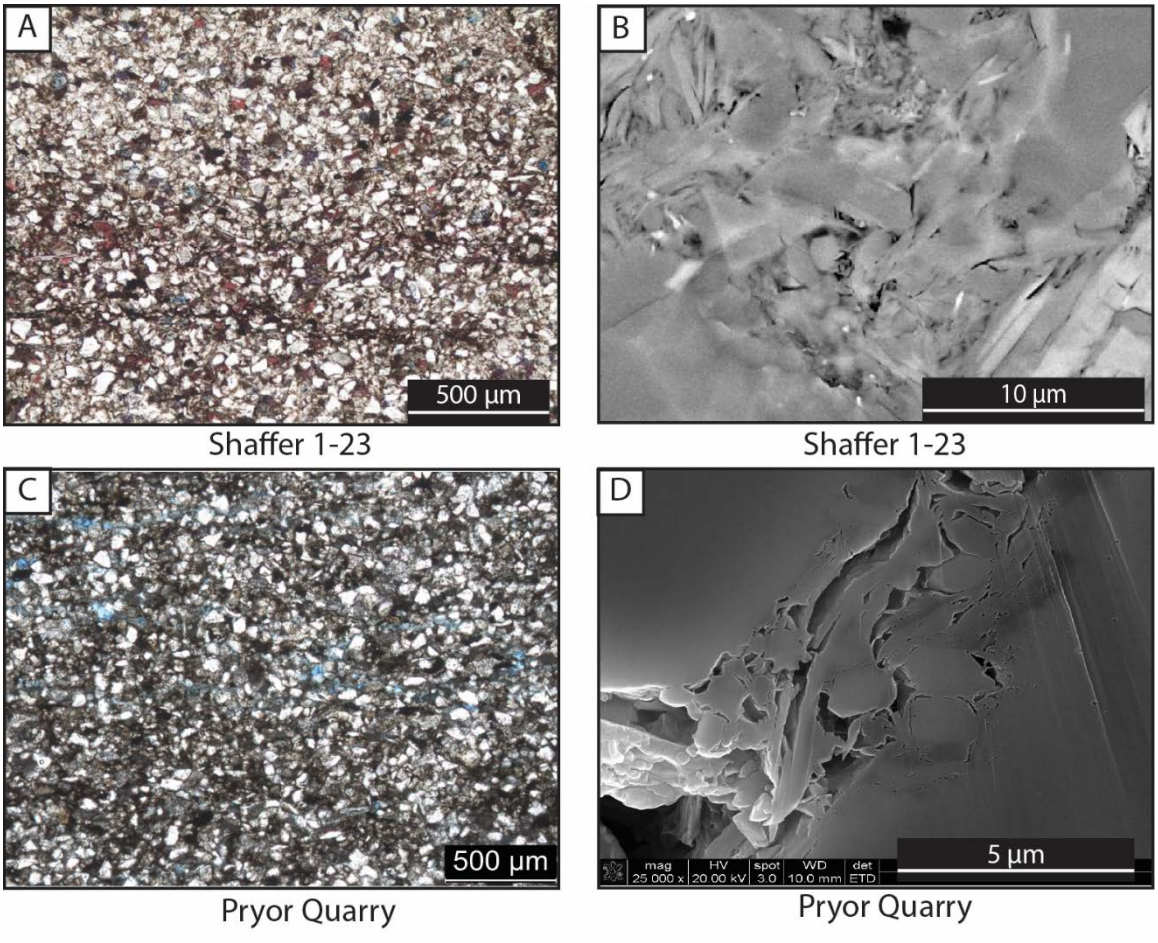

Figure 18: Comparison of the Shaffer 1-23 core from the STACK Play of Blaine County, OK and the Facies 1 reservoir of the Pryor Quarry. A: Stained "Argillaceous calcareous siltstone" photomicrograph from the Shaffer 1-23. Red stain indicates calcite, blue stain indicates dolomite. B: SEM photomicrograph from the Shaffer 1-23 showing pore-filling clay minerals ARROWS. C: Unstained Facies 1 reservoir of the Pryor Quarry. D: Pore-filling clay minerals with similar morphologies to those of the Shaffer 1-23 core.

Drone-Based Photogrammetry

Geologists have historically used photography and 3-D visualization to document, image, and map geological features. Recent advances in technology combining photogrammetric techniques with complex computer-based algorithms have provided the opportunity for large-scale data collection, modeling, and processing in relatively short periods of time (Bemis et al., 2014). Using photogrammetry, 3-D topographic information can be extracted from 2-D photographs. Modern photogrammetric modeling software is able to recognize millions of individual surface points across multiple aerial and orthogonal photos to build 3-D surfaces that can be textured and colored based on pixel values from the source photos. The resulting models exhibit high accuracy and precision in terms of both structure (surface dip angles) and image resolution.

One challenge of photogrammetry is the acquisition of high resolution orthogonal photos of inaccessible outcrops or structures. Sheer or unstable exposures provide difficulties for ground-based photography, while photos taken at high angles display significant distortion, which not only skews subject geometries but also inhibits accurate point matching of photos (Fitzgibbon, 2001). Recent innovations in civilian drone technology provide a fast, cost-effective method for acquiring high resolution orthogonal photos of high elevation subjects such as sheer outcrop walls. Drones offer the capability of taking both orthogonal and aerial photographs at multiple altitudes and distances. The greatest advantage of drone-based 3-D modeling over similar point cloud-based technology such as LiDAR (light detection and ranging) and TLS (terrestrial

laser scanning) is speed. In this study, an area of approximately 100,000 m^2 was captured at centimeter scale resolution in under 5 hours. More conventional techniques with poorer resolution and coverage may take weeks of data collection and processing to cover a similar study area (Bemis et al., 2014).

This study utilized a DJI Inspire 1 quadcopter drone (Figure 17, inset), which was equipped with a 12 megapixel camera mounted on a stabilizing gimbal. 950 aerial photos were taken at 10m (33 ft), 20m (67 ft), and 30m (100 ft) altitudes to provide high resolution and accurate point recognition and stitching. An additional 850 orthogonal photos were taken of the outcrop walls, resulting in a total of 1,800 photos. The Inspire 1 automatically geo-references every photo using on-board GPS, which significantly quickens processing times. Photos were imported into Agisoft Photoscan, a photogrammetric modeling software that creates 3-D orthomosaic models. Agisoft generates a point cloud from the photos, which it uses to create a solid 3-D mesh. The mesh is then colored and textured based on the photo EXIF data to produce the final model (Figure 19). The model can be more accurately scaled by inputting Ground Control Points (GCPs) or known distances. The model generated in this study exhibits a pixel size of 5 cm (higher resolutions are achievable through greater computing power) and a structural accuracy of $\pm 3^{o}$ dip.

The dense point cloud generated by the photogrammetric modeling was exported to Schlumberger's Petrel software as the base surface for geostatistical facies and porosity modeling.

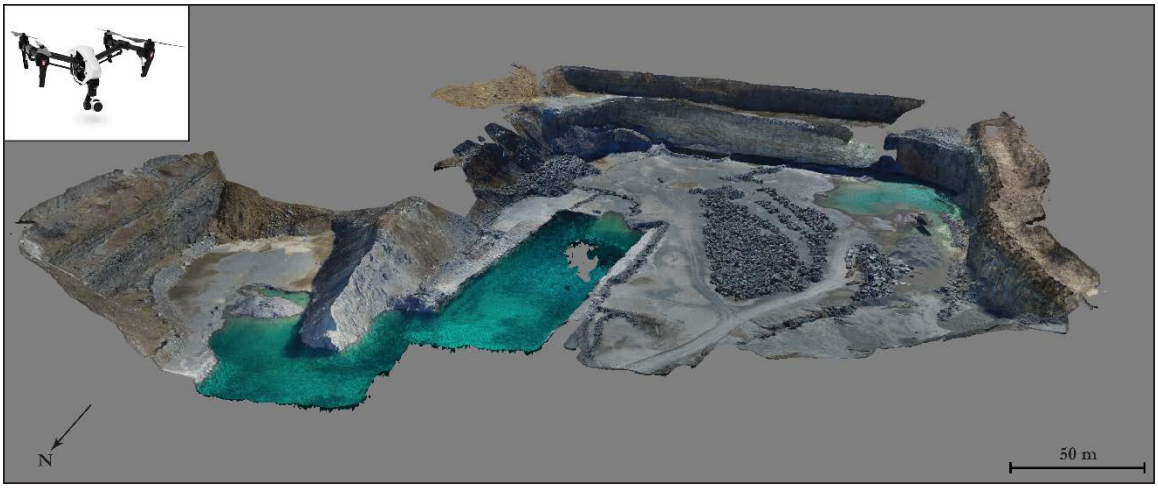

Figure 19: Agisoft 3-D photogrammetric outcrop model. The model is created from aerial and orthogonal photos stitched through point detection to create meshed and textured point clouds. Model holes are due to highly reflective surfaces, which are not well imaged using this technique. Inset: DJI Inspire 1 drone.

Petrel Modeling

Many previous Permian-aged carbonate outcrop modeling studies have covered large tracts of land, often kilometers in each direction (Goldhammer et al., 1993; Kerans et al., 1994; Jennings et al., 2000; Janson et al., 2007). While these studies are useful for modeling basin- or field-scale facies and geometrical relationships, the majority of Mid-Continent Mississippian outcrops consist of small-scale (less than 250m in length) two-dimensional road cut exposures. In addition to the size difference, the mixed carbonate-siliciclastic nature of the "Mississippi Lime" creates deviating facies and petrophysical trends from those of the oft-referenced Permian Guadalupe Mountain outcrops. The outcrop exposures at the Pryor Quarry provide a unique opportunity to study the facies and petrophysical relationships of Mid-Continent Mississippian carbonates on a three-dimensional scale. The quarry covers about 25 square acres (100,000 m^2), providing a basis for modeling rock characteristics over an area similar to that of average petroleum

well spacing (40 ac^2; 160,000 m^2). The 3-D grid used to create the model consisted of 8.2 million cells. Each cell was 2m in length, 2m in width, and 0.5m in height.

Measured sections completed in outcrop were input into Petrel as pseudo-wells. These wells were then populated with facies and porosity data input as ASCII well log files. Two additional pseudo-well data points were created for better facies control through Gigapan-based bedding tracing (Figure 20). By assuming that facies would remain consistent within a continuous bed at the relatively small scale of each outcrop wall, one additional measured section was approximated on the southern flank of Wall 3 and one between Walls 1 and 2. These additional points were not used for porosity modeling.

The reservoir model utilized the photogrammetric model as the base surface, as well as sequence boundary points that were collected using a GPS-enabled laser rangefinder. Convergent interpolation was used to interpolate boundary structure between data points. Four zones representing the four 4^{th}-order sequences observed in outcrop were created using proportional layering, which most closely reflected the outcrop geometries. By constraining the model using a sequence stratigraphic framework, the modeling algorithms model each sequence individually. This ensures that the algorithm only takes into consideration strata that were deposited over the same time interval.

1. Photography and Bedding Tracing

2. Digitized Outcrop Model

3. Sequence Stratigraphic Zone Constraints

4. Facies Modeling

5. Porosity Modeling

Figure 20: Workflow followed to transfer outcrop data to reservoir modeling software. Measured sections were augmented through bedding tracing to create additional facies data points. The digitized outcrop model was imported to Petrel as a point cloud-based surface. Sequence boundaries were used to constrain model zones. Facies and porosity models were created through an iterative comparison to measured sections to ensure accurate matching of simulated and real facies and porosity distributions.

Facies Modeling

Multiple iterations of both the facies and porosity models were created using various algorithms, variogram ranges, and nugget values (Table 1). Each iteration of the models was compared to the facies and porosity values observed in the outcrop walls. By comparing the modeled facies relationships and geometries to those actually present in the outcrop, modeling parameters could be iteratively modified to best fit the data. Truncated Gaussian simulation, sequential indicator simulation, and indicator kriging algorithms were tested for the most accurate representation of facies. Indicator kriging most accurately reflected the relationships present in outcrop, producing laterally continuous beds with gradational facies contacts, both laterally and vertically (Figure 21).

Algorithms	Horizontal Range	Vertical Range	Nugget
Kriging Interpolation	50	0.1	0.00001
Sequential Gaussian Simulation	100	0.3	0.0001
Gaussian Random Function Simulation	150	0.6	0.001
Sequential Indicator Simulation	200	1	0.01
Truncated Gaussian Simulation	250	2	0.1
Indicator Kriging	500	5	0.2
	1000	10	0.5

Table 1: Modeling parameters tested for both the facies and porosity models. A 500m horizontal variogram range, 2m vertical range, and 0.0001 nugget were ideal for facies modeling. A 100m horizontal range, 1m vertical range, and 0.01 nugget were ideal for porosity modeling.

Horizontally and vertical variogram ranges varied by sequence. Slight changes in horizontal variogram ranges were incorporated to reflect the pinching out of beds or facies between outcrop walls. A 500m horizontal variogram range and 0.6 m vertical range most accurately reflected the facies data obtained from outcrop. A 0.0001 nugget value created a facies model with minimal simulated variability within outcrop beds. At larger scales and with more data density, truncated Gaussian simulation may be more useful in simulating the inherent heterogeneity of field- or basin-scale carbonate systems, while indicator kriging seems to be more apt at creating the geometries observed on a 40 acre scale (Janson et al., 2007; Amour et al., 2012).

Porosity Modeling

Due to their high susceptibility to diagenetic alteration, porosity values within carbonate rocks are highly variable, often at sub-meter scales (Moore, 1989; Eisenberg et al., 1994; Kerans et al., 1994; James and Jones, 2015). The overall inaccessibility of the Pryor Quarry outcrops restricted core plug collection, resulting in sparse data coverage. A total of 40 data points were collected from the three walls, inhibiting the accuracy of porosity modeling. Much of the porosity variability within diagenetically altered carbonate formations can be represented using a higher nugget value (Pranter et al., 2005). However, the extensive diagenetic calcite cementation acted to occlude much of the expected porosity heterogeneity within the carbonates. A smaller nugget value more accurately modeled porosity within the siliciclastic facies. A final nugget value of 0.01 was chosen (Figure 21). A 100m horizontal variogram range and 0.3 m vertical range created porosity bodies whose geometries and continuity accurately reflected the expected geometries.

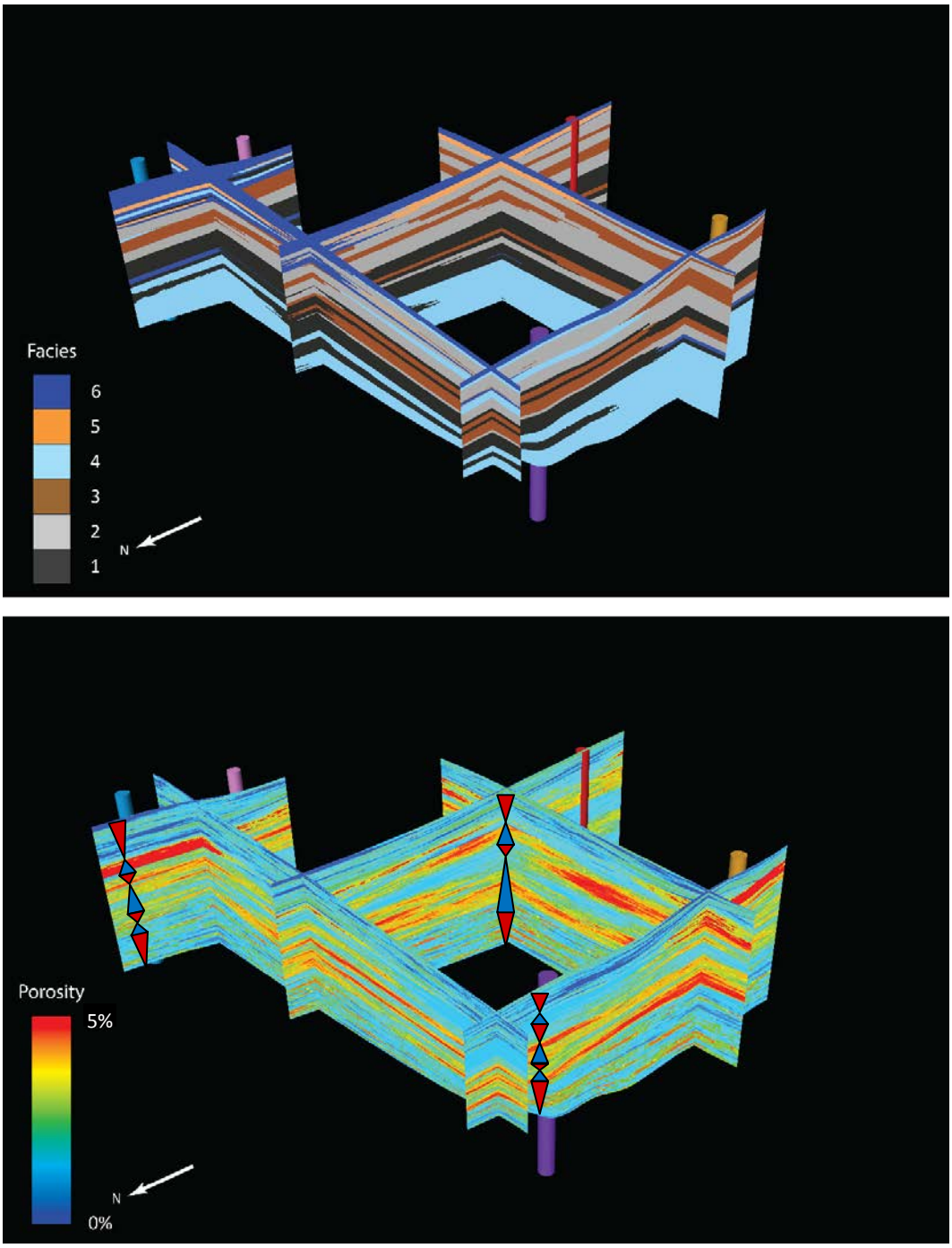

Figure 21: **A:** Petrel-based 3-D facies model of the Pryor Quarry created using an indicator kriging algorithm. **B:** 3-D model of porosity created using a Gaussian random function algorithm. The bulk of the reservoir quality lies within Facies 1 and 2, but varies significantly within beds. Facies 3-6 act as vertical and lateral seals, creating a highly compartmentalized reservoir. The model provides an excellent match between high porosity zones and transgressive systems tracts.

Multiple iterations of kriging interpolation, sequential Gaussian simulation (SGS), and Gaussian random function simulation (GRFS) were run using various nugget values. Both SGS and GRFS created porosity models with geologically reasonable porosity bodies, while kriging interpolation created a model with a false high degree of porosity continuity. The SGS and GRFS derived models correctly correlated high porosity values with Facies 1 and 2, while assigning low porosity values to Facies 4-6. Facies 3 porosity data was reflected with mixed results due to its proximity to large belts of Facies 1 and 2 high porosity zones. SGS and GRFS most accurately input porosity heterogeneity near extreme values, which closely simulating the variability created from zones of various degrees of cementation, fracturing, and dissolution that are expected in an exposed outcrop (Figure 22).

The modeled porosity values closely match the observed variability between facies and between outcrop walls. The majority of high porosity zones are contained within Facies 1 and 2, while Facies 3-6 are most commonly depicted as seals. The porosity model illustrates the vertical and lateral heterogeneity that are likely present in lithologically equivalent subsurface reservoirs. Reservoir compartmentalization within subsurface analogs such as the STACK Play is likely occurring vertically on a meter scale, and horizontally at a sub-reservoir scale. Petrophysical characteristics will vary both between and within facies, controlled by both depositional and diagenetic processes.

When extrapolating this model to the subsurface and to a field or basin scale, it is important to take the relationship of porosity and sequence stratigraphy into

consideration. While variability will exist within facies and sequences, the best reservoir quality will most likely be located at the base of sequences, which can be recognized in both core and well logs. The final porosity model shows an excellent correlation between transgressive facies and high porosity zones. By recognizing the relationship of reservoir quality to sequence stratigraphy, the vertical and lateral compartmentalization that exists within strata and between wells can be more accurately predicted, as can volumetric calculations that predict overall recoveries.

Permeability

Permeability values collected from the Pryor Quarry were extremely low, ranging from less than .0001 mD to .007 mD. These low values are likely due to extensive calcite cementation within Facies 2-6, and to the occlusion of pore throats and pore-connecting fractures by clay minerals in Facies 1 and 2. Due to the minimal range in values, permeability is considered to have a negligible effect on relative reservoir quality between facies. In this case, modeling of permeability, typically an important step in determining reservoir potential, was considered ineffectual.

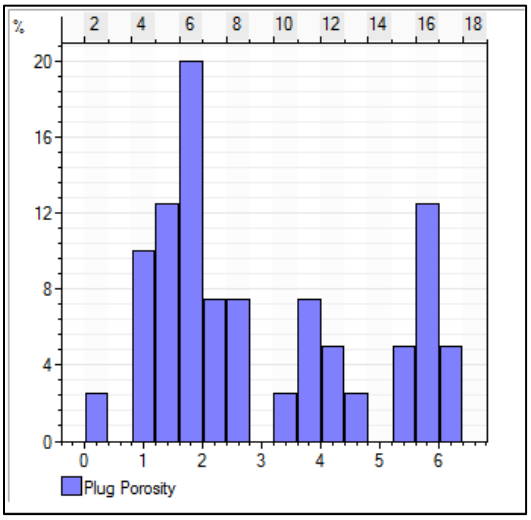

Porosity Input Histogram

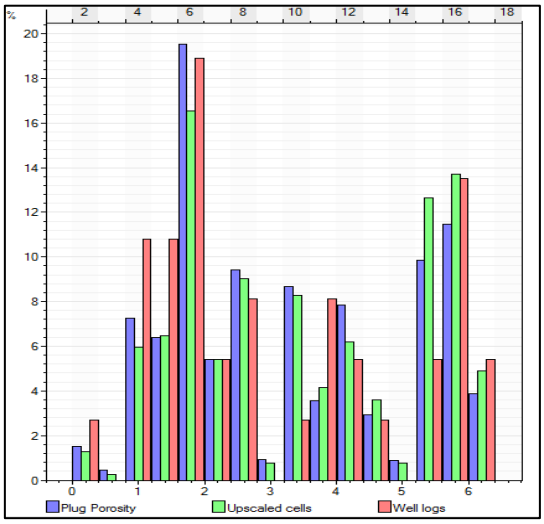

Porosity Output Histogram

Figure 22: Input and output histograms showing the distribution of porosity data before and after modeling. Both the sequential Gaussian and Gaussian random function simulations create greater degrees of heterogeneity near extreme data values.

Summary

Six lithofacies were identified within the Moorefield and Hindsville Formations in Pryor Creek, Oklahoma. These facies were deposited within a distally-steepened ramp environment, ranging from outer ramp to ramp crest shoal environments.

The quartz mudstone-wacke facies acts as the main reservoir facies within the outcrop. This facies is a direct lithological analog to similar reservoir types within the STACK play of Oklahoma. Reservoir quality is likely a function of depositional clay content. Higher clay content and clay rims likely act as an inhibitor to diagenetic calcite cementation. Porosity exhibits an inverse relationship with the percentage of calcite within a sample.

Using a quadcopter drone, a high-resolution 3D photogrammetric model was created of the Pryor Creek quarry that provided centimeter-scale resolution of the study area that is easily manipulated and exportable to modeling software. The use of drone-based photogrammetry provides a distinct speed and time advantage over more tradition LiDAR-based point cloud collection, while also providing unparalleled ease of access to unstable or sheer outcrop walls for high-resolution photography and recognition of small-scale sedimentary features. The photogrammetric model can be easily incorporated with petrophysical data for use in reservoir modeling.

Using an idealized vertical stacking pattern and previously defined conodont biostratigraphic data, two 3rd-order sequences were identified, comprised of three to four 4th-order high frequency sequences, which provided constraints for reservoir modeling. The development of a vertical stacking pattern and sequence stratigraphic

framework allows for the extrapolation of reservoir data away from outcrop or core locations. The best reservoir quality in the Mid-Continent Meramecian strata will likely be found at the base of sequences, and can be predicted through the use of sequence stratigraphy and the recognition of the Facies 1 log signature.

An indicator kriging algorithm using a horizontal variogram range of 500m, vertical range of 0.6m, and nugget of 0.0001 most accurately recreates the facies relationships present at the Pryor Quarry. Both sequential Gaussian simulation and Gaussian random function simulation create reasonable approximations of porosity relationships. A horizontal variogram range of 100m, vertical range of 0.3m, and nugget of 0.01 most accurately recreate the porosity data from the Pryor Quarry.

CHAPTER III

EXTENDED RESERVOIR MODELING PARAMETERS

While subsurface models of the "Mississippi Limestone" have been created through well log interpolations (Costello, 2014), an outcrop-based model ensures that modeling parameters accurately reflect the actual facies and petrophysical relationships present and minimizes the likelihood of false data.

The initial step for creating the model was to import the base quarry surface from the Agisoft drone-derived model (Figure 22). The dense point cloud was converted from the local GPS coordinate system (UTM 15N, EPSG::26915) to a local coordinate system, exported as an ASCII point file, and was used as the main input for creating the base surface of the model. Vertical measured sections were treated as pseudo-wells, imported based on location and depth from the top of the quarry. Pseudo-wells were then populated with facies and porosity data. Facies were input on a simple 1 (Quartz Mudstone-Wacke) to 6 (Skeletal Packstone-Grainstone) scale. Porosity was input on a 0-6% scale.

Sequence stratigraphic surfaces were digitized by a combination of laser rangefinder and Agisoft marker points. Boundaries included 3rd-order sequence boundaries and intra-sequence TST-HST boundaries. These were delineated in the field using a GPS-capable laser rangefinder that calculated the GPS offset of the target relative to the rangefinder's location. This allowed for the rangefinder coordinates to be calibrated to the coordinate system of the Agisoft model. Rangefinder sequence boundary coordinates were confirmed in both Agisoft and Petrel by comparing their plotted locations to actual locations documented through field photography.

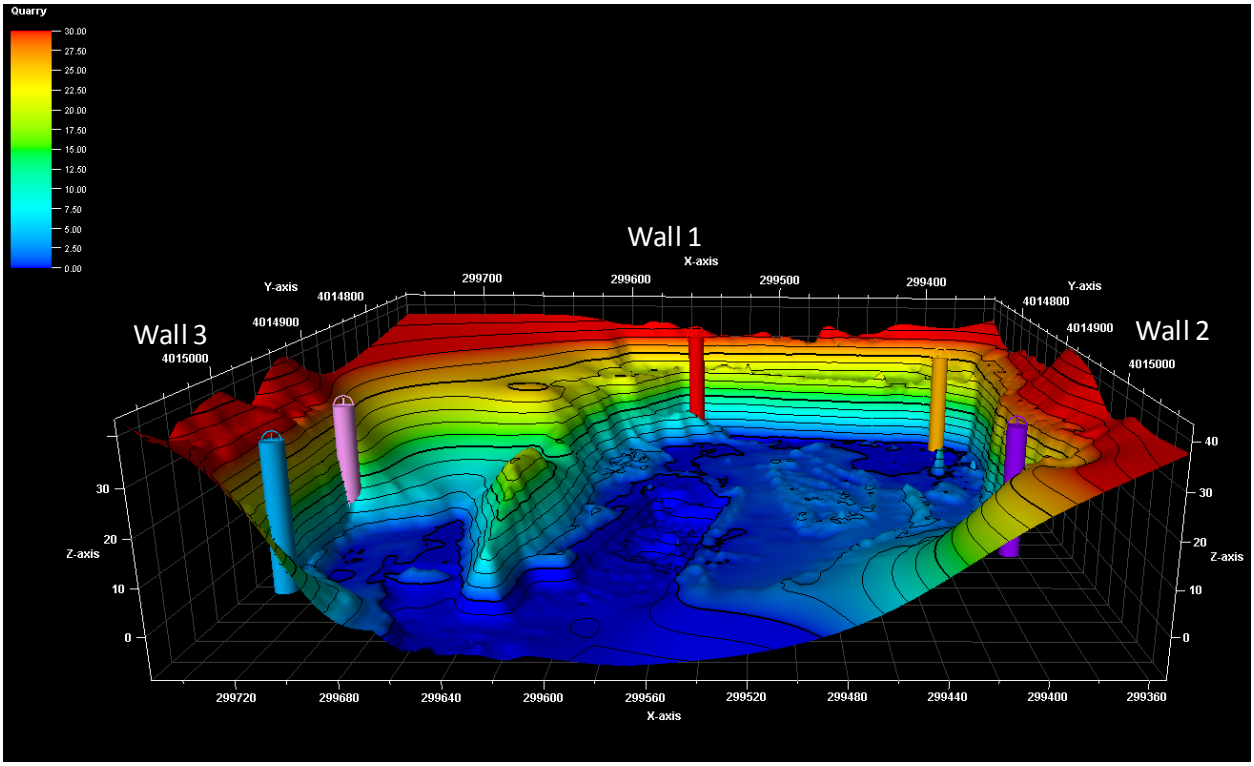

Figure 23: Base surface used to constrain Petrel reservoir modeling. The surface was sourced from the Agisoft point cloud and used to create a contoured Petrel surface. This surface was then used as the bounding surface for porosity and facies modeling.

Boundary points were collected at regular intervals along all three outcrop walls, providing consistent coverage of the modeled area. By combining the rangefinder points and the Agisoft-derived boundary surface, sequence boundaries were able to be interpolated with confidence. The convergent interpolation algorithm was used to interpolate boundary structure between data points. This algorithm provides greater detail near data points and smoother geometries away from data (Figure 23). Convergent interpolation works well for the outcrop given the three-sided data control and relatively small interpolated volume between walls.

When generating model layers bounded by sequence horizons, several zone division options were considered. Proportional layering was used for all but one zone, as it most accurately represented the geometries present in outcrop. The exception was the S3 TST horizon, which was made to follow the erosive surface located between the Moorefield and Hindsville Formations. Zones contained a range of layers, from 10 to 75, based on the thickness of each zone (Figure 24).

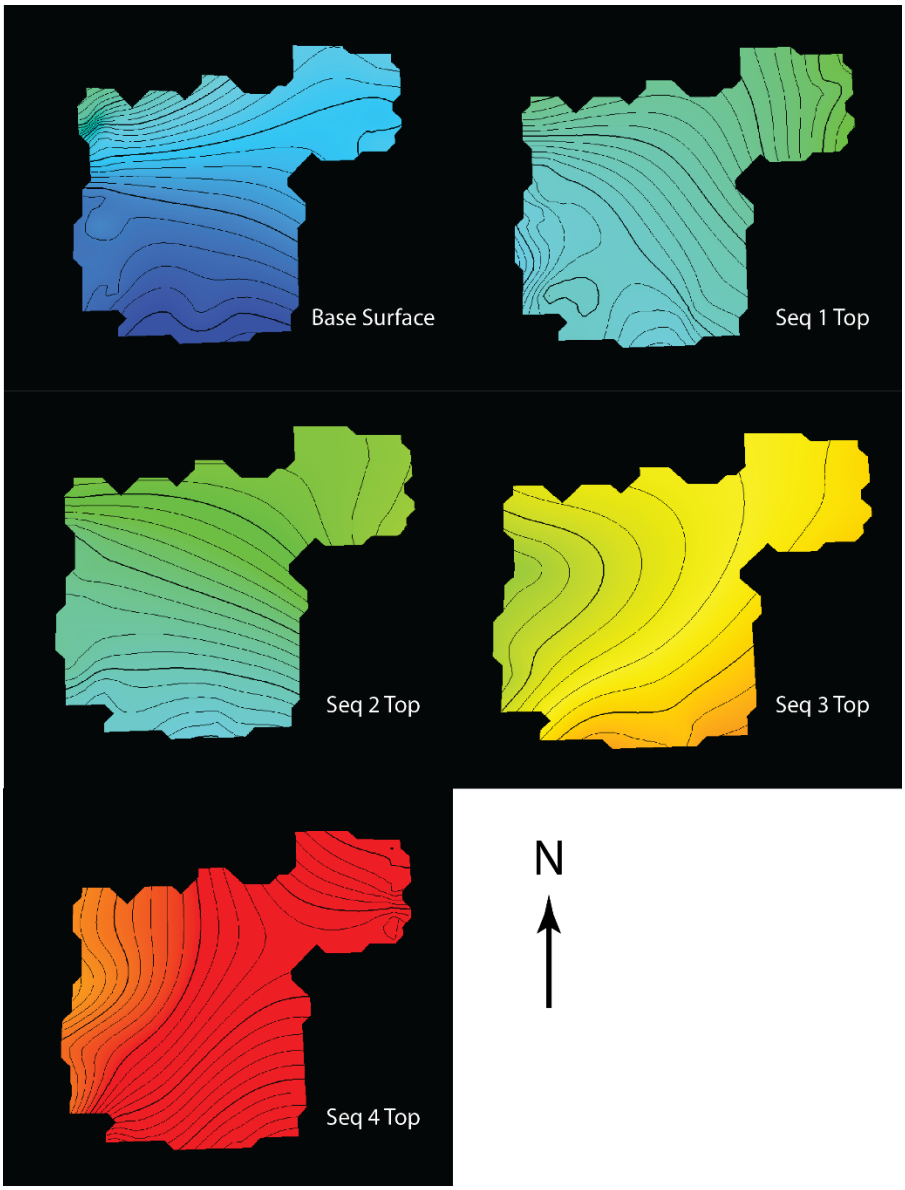

Figure 24: Structural contour maps of the Pryor Quarry showing the sequence stratigraphic surfaces used to create modeling zones. Surfaces were interpolated between points using a convergent interpolation algorithm. By constraining facies and petrophysical models with chronostratigraphic surfaces, tighter constraints are placed on facies and petrophysical distributions to create more geologically accurate lateral and vertical parameter relationships.

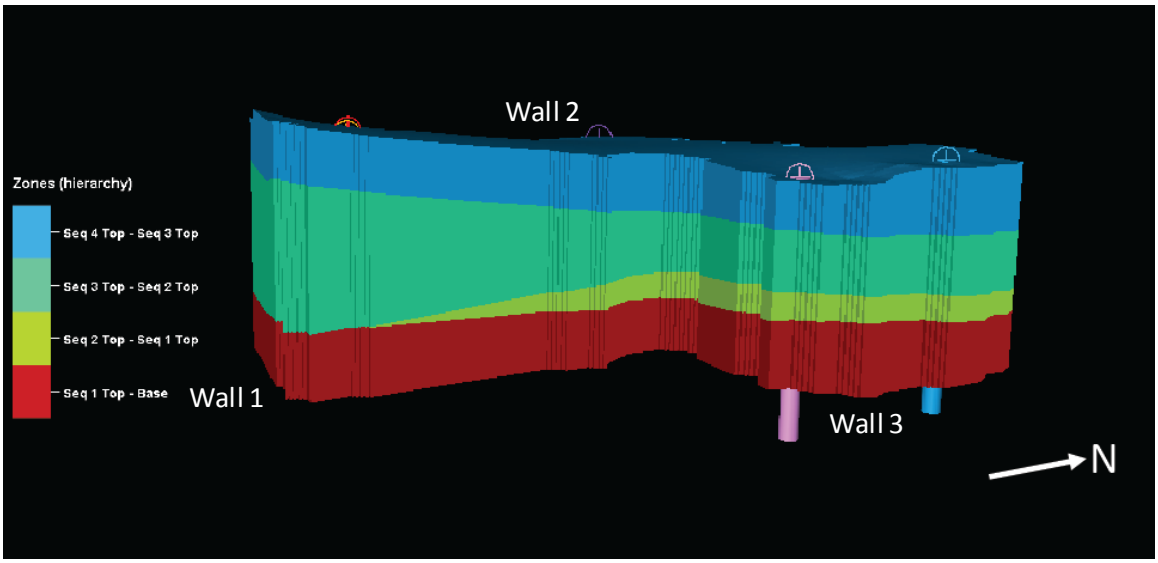

Figure 25: Zones used for reservoir modeling. Zone boundaries were picked based on sequence boundaries. Proportional layering was used in all but one zone. One zone used Follow Surface layering, to reflect erosion.

Populating the 3-D volume with facies and petrophysical data is an iterative process, requiring the testing of multiple algorithms and variograms to find the best fit for the actual geological relationships present in outcrop. By constraining the model with sequence stratigraphic boundaries, each sequence can be modeled independently. This allows rocks deposited under different conditions, different times, and with different geometries to be accurately reflected without influence of geologically un-related strata. For example, skeletal shoals in S3 HST will have different lateral and vertical geometries than the siltstones of S2 TST.

Three algorithms were tested when modeling facies: indicator kriging, truncated Gaussian simulation, and sequential indicator simulation. Indicator kriging is a deterministic modeling simulation that estimates a value at a given location based on its distance from known data points and the magnitude of said points. It produces a model with little simulated heterogeneity, relying on the input data and any user-input

anisotropy trends. Truncated Gaussian simulation is a stochastic method that relies on facies probability mapping. These maps consist of the percentages of each facies within each pseudo-well, mapped as a surface. Greater percentages of certain facies appear as higher values. These create a higher likelihood of certain facies appearing near data points where they occur more commonly. Truncated Gaussian simulation is useful for systems without highly geometrical facies bodies (Pyrcz and Deutsch, 2014), where facies do not sharply contrast. Sequential indicator simulation is a stochastic method that creates multiple realizations by utilizing indicator kriging at each model node (Pyrcz and Deutsch, 2014). It is useful in representing the probability of facies transition at a given point.

In addition to algorithm testing, multiple variogram range and nugget values were tested to reproduce outcrop geometries and bed continuity. Larger horizontal and vertical range values resulted in more continuous facies geometries, while lower nugget values reduced small scale variability within the models (Figure 25). Sequential indicator simulation produced highly variable and non-geometric facies assemblages at every tested range and nugget value.

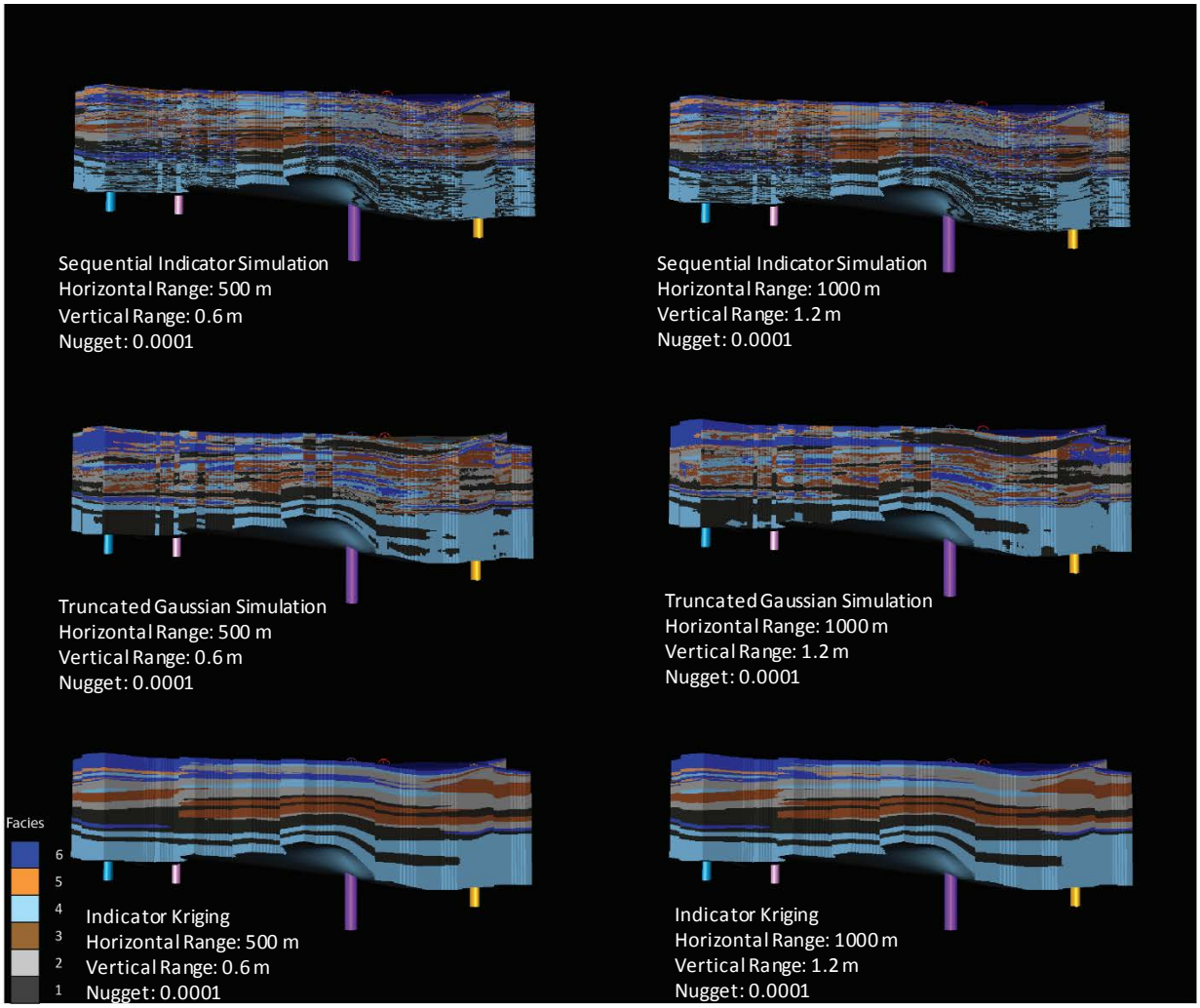

Figure 26: Iterations of facies modeling. The upper two models reflect facies models created using a sequential indicator simulation. The middle two models used truncated Gaussian simulation, while the lower two models used indicator kriging. Indicator kriging provides a model that most accurately reflects the patterns observed in outcrop.

The truncated Gaussian simulation produced more laterally continuous facies, but introduced many lens-like facies bodies that are not actually present in the outcrops. Larger horizontal and vertical range values produced more geologically reasonable facies geometries, but would be more suited to a field or basin scale. Truncated Gaussian simulation was used for S1 TST, which contains some intermixing of Facies 1 and 4.

Indicator kriging produced laterally continuous beds with gradual facies contacts both vertically and laterally. Lower range values created holes in the data, but larger values produced geologically sound geometries that most accurately represent those found in outcrop.

At small scales, indicator kriging appears to be the most geologically sound algorithm for facies modeling, while truncated Gaussian simulation is more suited to larger scale modeling. Stochastic simulations such as sequential Gaussian simulation are the mostly widely used in subsurface modeling due to its ability to simulate small-scale uncertainties (Janson et al., 2007). While sequential indicator simulation also simulates small-scale uncertainties, the geometries of those features seem to be geologically unreasonable.

Porosity modeling

Due to their high susceptibility to diagenetic alteration, porosity values within carbonate rocks are highly variable, often at sub-meter scales (Moore, 1989; Eisenberg et al., 1994; Kerans et al., 1994; James and Jones, 2015). Both the carbonate and siliciclastic strata present at the Pryor Quarry outcrops have undergone extensive diagenetic alteration in the form of multiple calcite and silica cementation events, fracturing, and recent exposure dissolution.

The Gaussian random function simulation was chosen for porosity modeling for its ability to produce variability while accurately reflecting the geometries of facies-controlled porosity zones observed within outcrop (Figure 26). Much of the small scale porosity variability within diagenetically altered carbonate formations can be

represented using a higher nugget value (Pranter et al., 2005). Multiple iterations of the Gaussian random function simulation were run using various nugget values. A final nugget value of 0.01 was chosen.

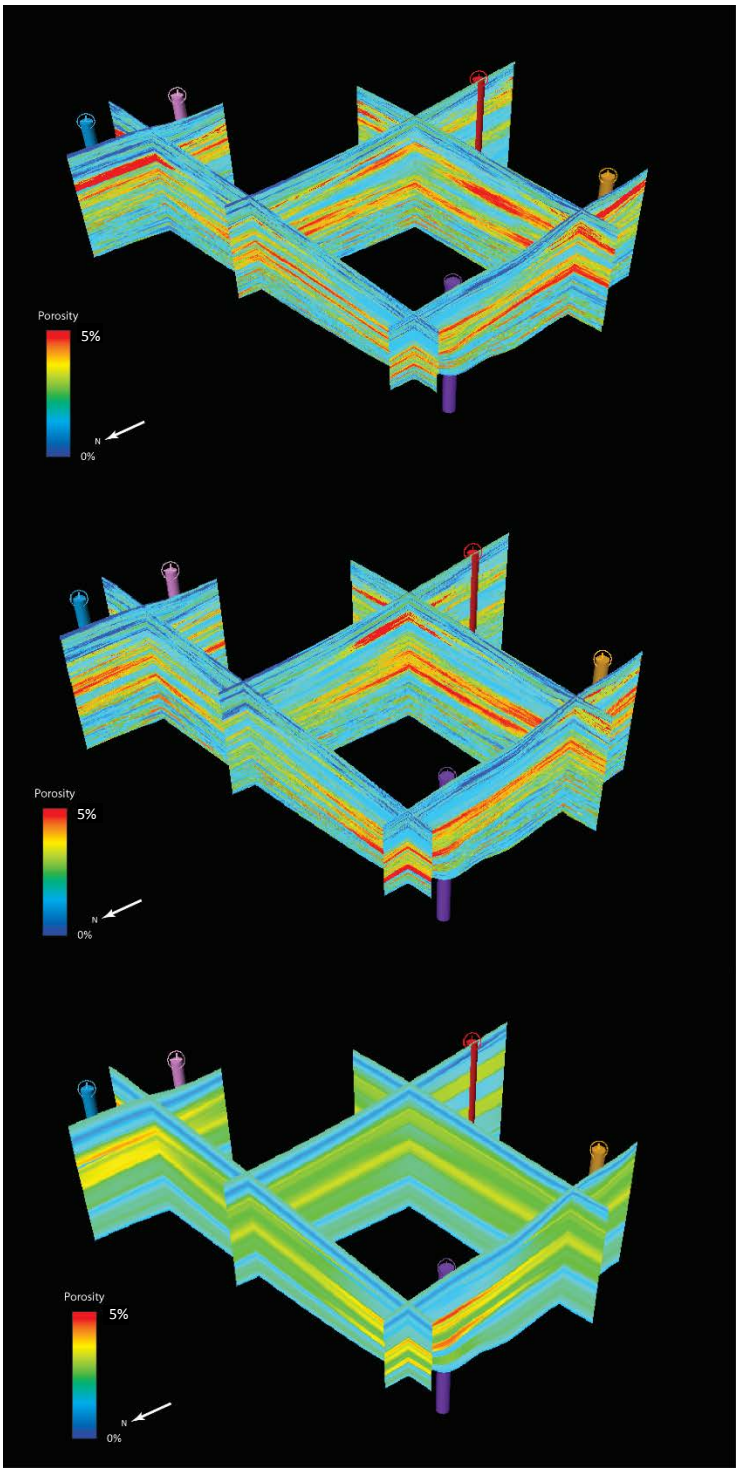

Figure 27: Various porosity modeling algorithms. **A:** Gaussian random function simulation. **B**: Sequential Gaussian simulation. **C:** Kriging interpolation. Kriging interpolation provides the least geologically reasonable representation of porosity, imparting little to no internal heterogeneity with respect to porosity.

CHAPTER IV

SUMMARY AND CONCLUSIONS

This study integrated multiple datasets and techniques to identify likely controls on facies deposition and distribution, depositional geometries, and reservoir development within the Mississippian Moorefield and Hindsville Formations. Thin sections and core plugs were used to identify distinct facies and their petrophysical characteristics. An idealized vertical facies stacking pattern and sedimentologically significant surfaces were incorporated to create a sequence stratigraphic framework of the three outcropping walls. This data was then integrated with gigapixel and drone photography to develop 3-D geostatistical models of outcrop facies and porosity. The key conclusions of this study are as follows:

1. Three carbonate and three siliciclastic depositional facies were identified from thin section and hand sample, reflecting changes in dominant sedimentation type.
2. Siliciclastic sedimentation was likely dominant during lowstands and transgressions of sea level, while carbonate sedimentation was likely dominant during highstand. Two partial 3rd-order sequences were identified using a vertical

facies stacking pattern. 3rd-order sequences were constrained using conodont biostratigraphy. Three to four 4th-order high frequency sequences are superimposed upon the 3rd-order sequences.

3. Sequence stratigraphy can be used as a predictive tool within the study area. The best reservoir quality in the Mid-Continent Meramecian strata will likely be found at the base of sequences, and can be predicted through the use of sequence stratigraphy and the recognition of the Facies 1 log signature.
4. Deposition of the Moorefield and Hindsville Formations likely occurred near the ramp crest of a distally-steepened ramp. This is inferred from the presence of a siliciclastic bar and carbonate shoal, as well as the close juxtaposition of deep water and shallow water facies.
5. Reservoir quality seems to hinge on the effects of diagenetic calcite cementation, which affects every facies but Facies 1, in which depositional and authigenic clay minerals likely inhibit calcite cements. Facies 1 provides the highest reservoir quality, while the highly cemented carbonate facies (4-6) act as the primary seals to vertical fluid flow.
6. Drone photogrammetry provides a fast, simple method to capture outcrop geometries in three dimensions, then directly import them to modeling software.
7. An indicator kriging algorithm using a horizontal variogram range of 500m, vertical range of 0.6m, and nugget of 0.0001 most accurately recreates the facies relationships present at the Pryor Quarry. Both sequential Gaussian simulation

and Gaussian random function simulation create reasonable approximations of porosity relationships. A horizontal variogram range of 100m, vertical range of 0.3m, and nugget of 0.01 most accurately recreate the porosity data from the Pryor Quarry.

8. The Shaffer 1-23 core provides a subsurface lithological analog that ties the siliciclastic lithologies seen at the Pryor Quarry to those observed in the STACK Play of the Anadarko Basin, indicating that siliciclastic deposition was widespread across Oklahoma at times during the Mississippian.

REFERENCES

Ahr, W.M., 1973, The carbonate ramp: an alternative to the shelf model: GCAGS Transactions, v. 23, p. 221-225.

Amour, F., Mutti, M., Christ, C., Immenhauser, A., Benson, G., Agar, S., Tomas, S., Kabiri, L., 2013, Outcrop analog for an oolitic carbonate reservoir: A scale-dependent geologic modeling approach based on stratigraphic hierarchy: AAPG Bulletin, v. 97, no. 5, p. 845-871, doi 10.1306/10231212039.

Bemis, S., Micklethwaite, S., Turner, D., James, M., Akciz, S., Thiele, S., Bangash, H.A., 2014, Ground-based and UAV-Based photogrammetry: A multi-scale, high-resolution mapping tool for structural geology and paleoseismology: Journal of Structural Geology, v. 69, p. 163-178, doi 10.1016/j.jsg.2014.10.007.

Blakey, Ron, 2013, Paleogeography and Geologic Evolution of North America, http://www2.nau.edu/rcb7/nam.html. Accessed October 2015.

Boardman, D.R. II, Mazzullo, S., Wilhite, B., Puckette, J., Thompson, T., and Woolsey, I., 2010, Diachronous prograding carbonate wedges from the Burlington Shelf tot the southern distal shelf/basin in the southern flanks of the Ozarks: Abstracts with Programs, Joint North-Central and South-Central Meeting, Geological Society of America, v. 42, no. 2, p. 41.

Buggisch, Werner, Joachimski, Michael M., Sevastopulo, George, and Morrow, Jared R., 2008, Mississippian δ 13Ccarb and Conodont Apatite δ18O Records – Their Relation to the Late Palaeozoic Glaciation, Palaeogeography, Palaeoclimatology, Palaeoecology 268, p. 273-292.

Burchette, T.P. and Wright, V.P., 1992, Carbonate ramp depositional systems: Sedimentary Geology, v. 79, p. 3-57.

Buxton, T.M., and Sibley, D.F., 1981, Pressure solution features in a shallow buried limestone: Journal of Sedimentary Petrology, v. 51, no. 1, p. 19-26.

CoreLab, 2015. Mississippi Lime geological, petrophysical, and completions study, http://www.corelab.com/irs/studies/mississippi-lime. Accessed Nov 2015.

Childress, M., 2015, High resolution sequence stratigraphic architecture of a Mid-Continent Mississippian outcrop in southwest Missouri, Master's Thesis, Oklahoma State University, Stillwater, OK, 266 p.

Childress, M. and Grammer, G.M., 2015, High Resolution Sequence Stratigraphic Architecture Of A Mid-Continent Mississippian Outcrop In Southwest Missouri , Shale Shaker, July/August, p. 206 - 234.

Costello, Dan, 2014. Use of reservoir models and dynamic simulation in development of Mississippian. AAPG Search and Discovery Article #41314.

Curtis, Doris M. and Champlin, Stephen C., 1959, Depositional Environments of Mississippian Limestones of Oklahoma, Tulsa Geological Society Digest, v. 27, no. 1, p. 90-103.

Dixon, S.A., Summers, D.A., and Surdam, R.C., 1989, Diagenesis and preservation of porosity in Norphlet Formation (Upper Jurassic), Southern Alabama: AAPG Bulletin, v. 73, p. 707-728.

Dott, R.H. Jr., and Bourgeois, J., 1982, Hummocky stratification: Significance of its variable bedding sequences: GSA Bulletin, v. 93, p. 663-680.

Ehrenberg, S., Svånå, T., 2000, Use of spectral gamma-ray signature to interpret stratigraphic surfaces in carbonate strata: An example from the Finnmark carbonate platform (Carboniferous-Permian), Barents Sea: AAPG Bulletin, v.85, no. 2, p. 295-308.

Eisenberg, R.A., Harris, P.M., Grant, C.W., Goggin, D.J., Conner, F.J., 1994, Modeling reservoir heterogeneity within outer ramp carbonate facies using an outcrop analog, San Andres Formation of the Permian Basin: AAPG Bulletin, v. 78, no. 9, p. 1337-1359.

Fitzgibbon, A.W., 2001, Simultaneous linear estimation of multiple view geometry and lens distortion: Proceedings of the IEEE Conference on Computer Vision and Pattern Recognition, p. 125-132.

Flinton, K.C., 2016, The effects of high-frequency cyclicity on reservoir characteristics of the "Mississippian Limestone", Anadarko Basin, Kingfisher County, Oklahoma, Master's Thesis, Oklahoma State University, Stillwater, OK, 118 p.

Grammer, G. M., P. M. Harris, G. P. Eberli, 2004, Integration of Outcrop and Modern Analogs in Reservoir Modeling: Overview with Examples from the Bahamas, in G. M. Grammer, P. M. Harris, and G. P. Eberli, eds., Integration of Outcrop and Modern Analogs in Reservoir Modeling: American Association of Petroleum Geologists Memoir 80, p. 1-22.

Handford, C.R. and Loucks, R.G., Carbonate depositional sequences and systems tracts – responses of carbonate platforms to relative sea level changes: AAPG Memoir 57: Carbonate Sequence Stratigraphy, p. 3-42.

Haq, B. U., and Schutter, S. R., 2008, A Chronology of Paleozoic Sea-Level Changes, Science, v. 322, p. 64-68.

Gaillard, C., and Racheboeuf, P. R., 2006, Trace fossils from nearshore to offshore environments: Lower Devonian of Bolivia: Journal of Paleontology, v. 80, no. 6, p. 1205-1226.

Godwin, C., 2010, Review of the Upper Mississippian Mayes Group (Meramecian and Chesterian) of northeastern Oklahoma, GSA Abstracts with Programs, v. 42, no. 2, p. 41.

Goldhammer, R.K., Oswald, E.J., and Dunn, P.A., 1991. Hierarchy of stratigraphic forcing: Example from Middle Pennsylvanian shelf carbonates of the Paradox Basin: in Fraaseen, E. K., Watney, W. L., Kendall, G.C.St.C., and Ross, W., eds., Sedimentary Modeling: Computer Simulations and Methods for Improved Parameter Definition: Kansas Geological Survey Bulletin, v. 233, p. 361-414

Goldhammer, R.K., Lehmann, P.J., and Dunn, P.A., 1993, The origin of high-frequency platform carbonate cycles and third-order sequences (Lower Ordovician El Paso Gp, west Texas): Constraints from outcrop data and stratigraphic modeling: Journal of Sedimentary Petrology, v. 63, no. 3, p. 318-359.

Grammer, G.M., Eberli, G.P., Van Buchem, F.S.P., Stevenson, G.M., and Homewood, P., 1996, Application of high-resolution sequence stratigraphy to evaluate lateral variability in outcrop and subsurface – Desert Creek and Ismay intervals, Paradox Basin: *in* Paleozoic Systems of the Rocky Mountain Region, p. 235-266.

Handford, C.R., 1986, Facies and bedding sequences in shelf-storm-deposited carbonates Fayetteville shale and Pitkin Limestone (Mississippian), Arkansas: Journal of Sedimentary Petrology, v. 56, p. 123-137.

Huffman, George G., 1958, Geology of the Ozark Uplift, Northeastern Oklahoma, Oklahoma City Geological Society, The Shale Shaker Digest I, v. I-V, p. 36-42.

James, N.P., and Jones, B., 2015, Origin of carbonate sedimentary rocks, American Geophysical Union, West Sussex, John Wiley and Sons, 464 p.

Janson, X., Kerans, C., Bellian, J.A., and Fitchen, W., 2007, Three-dimensional geological and synthetic seismic model of Early Permian redeposited basinal carbonate deposits, Victorio Canyon, west Texas: AAPG Bulletin, v. 91, no. 10, p. 1405-1436, doi 10.1306/05210705.

Jennings, J.W. Jr., Ruppel, S.C., and Ward, W.B., 2000, Geostatistical analysis of permeability data and modeling of fluid-flow effects in carbonate outcrops: Society of Petroleum Engineers Reservoir Evaluation and Engineering, v. 3, no. 4, p. 292-303.

Kerans, C., 1988, Karst-controlled reservoir heterogeneity in Ellenburger Group carbonates of west Texas: AAPG Bulletin, v. 72, no. 10, p. 1160-1183.

Kerans, C., Lucia, F.J., and Senger, R.K., 1994, Integrated characterization of carbonate ramp reservoirs using Permian San Andres Formation outcrop analogs: AAPG Bulletin, v. 78, no. 2, p. 181-216

Kerans, C., and Tinker, S., 1997, Sequence Stratigraphy and Characterization of C arbonate Reservoirs: SEPM, Short Course, no. 40, 130 p.

Knauth, L.P., 1979, A model for the origin of chert in limestone: Geology, v. 7, p. 274-277.

Lane, H. R., and DeKyser, T. L., 1980, Paleogeography of the Late Early Mississippian (Tournaisian) in the Central and Southwestern United States, Paleozoic Paleogeography of West-Central United States: Rocky Mountain Paleogeography Symposium 1, p. 149-162.

Leblanc, S.L., and Grammer, G.M., 2014, High resolution sequence stratigraphy and reservoir characterization of the Mississippian Lime in northeastern Oklahoma: AAPG Search and Discovery Article #90189, Abstract.

Lucia, F. J., Kerans, C., and Singer, R.K., 1992, Defining flow units in dolomitized carbonate-ramp reservoirs: 67th Society of Petroleum Engineers Annual Technical Conference and Exhibition, Washington, D.C., October 4–7, SPE Paper 24702, p. 399–406.

Lucia, F. J., Kerans, C., and Jennings, J.W. Jr., 2003, Carbonate reservoir characterization: Journal of Petroleum Technology, v. 55, no. 6, p. 70-72.

Mazzullo, S.J., and Reid, A.M., 1989, Lower Permian platform and basin depositional systems, northern Midland Basin, Texas: *in* SEPM Special Publication No. 44, p. 305-320.

Mazzullo, S.J., Wilhite, Brian W., and Woolsey, I. Wayne, 2009, Rhythmic Carbonate Versus Spiculite Deposition in Mississippian Hydrocarbon Reservoirs in the Mid-Continent USA: Causative Factors and Resulting Reservoir Petrophysical Attributes, AAPG Search and Discovery Article #10209, 6 p.

Mazzullo, S.J., 2013, Boardman, D.R., II, Wilhite, B.W., Morris, B.T., 2013 Revisions of outcrop lithostratigraphic nomenclature in the Lower to Middle Mississippian Subsystem (Kinderhookian to Basal Meramecian Series) along the shelf-edge in southwest Missouri, northwest Arkansas, and northeast Oklahoma: Shale Shaker Digest, v. 63, p. 414-454.

McBride, E.F., 1985, Sandstone diagenesis: SEPM Short Course Notes, 75p.

McCubbin, D.G., 1981, Barrier-island and strand-plain facies: AAPG Memoir 31: Sandstone Depositional Environments, p. 249-279.

Moraes, M.A.S. and De Ros, L.F., 1990, Infiltrated clays in fluvial Jurassic sandstones of Reconcavo Basin, northeastern Brazil: Journal of Sedimentary Petrology, v. 60, no. 6, p. 809-819.

Moore, C.H., 1989, Carbonate diagenesis and porosity, Amsterdam, Elsevier Science B.V., 337 p.

Northcutt, R. A., and Campbell, J. A., 1996, Geologic Provinces of Oklahoma, Transactions of the 1995 AAPG Mid-Continent Section Meeting, 1996, p. 128-134.

Penland, S., Boyd, R., and Suter, J.R., 1988, Transgressive depositional systems of the Mississippi delta plain: A model for barrier shoreline and shelf sand development: Journal of Sedimentary Petrology, v. 58, no. 6, p. 932-949.

Pittman, E.D. and Lumsden, D.N., 1968, Relationship between chlorite coatings on quartz grains and porosity, Spiro Sand, Oklahoma: Journal of Sedimentary Petrology, v. 38, p. 668-670.

Pranter, M.J., Hirstius, C.B., and Budd, D.A., 2005, Scales of lateral petrophysical heterogeneity in dolomite lithofacies as determined from outcrop analogs: Implications for 3-D reservoir modeling: AAPG Bulletin, v. 89, no. 5, p. 645-662, doi 10.1306/11300404049.

Price, B.J., 2016, High resolution sequence stratigraphic architecture and reservoir characterization of the Mississippian Burlington/Keokuk Formation, northwestern Arkansas, Master's Thesis, Oklahoma State University, Stillwater, OK, 144 p.

Purdue, E.F., Adams, G.I., and Ulrich, E.O., 1904, Zinc and lead deposits of northern Arkansas, with a section on the determination and correlation of formations: USGS Report, no. 24, 118 p.

Purdue, A.H., 1907, Description of the Winslow quadrangle: USGS Winslow Folio, 6 p.

Purdue, A.H., and Miser, H.D., 1916. Descriptions of the Eureka Springs and Harrison quadrangles. U.S. Geological Survey Atlas, No. 202.

Pyrcz, M. J. and Deutsch, C. V., 2014, Geostatistical reservoir modeling, Oxford University Press, Oxford, N.Y., 448 p.

Read, J.F., 1995, Overview of Carbonate Platform Sequences, Cycle Stratigraphy and Reservoirs in Greenhouse and Icehouse Worlds, In: Read, J. F., Kerans, C., Weber, L. J., Sarg, J. F., and Wright, F. M. (eds.), Milankovitch Sea Level Changes, Cycles, and Reservoirs on Carbonate Platforms in Greenhouse and Ice-House Worlds: SEPM Short Course 35, p. 1-102.

Ross, C. A., and Ross, J. R., 1988, Late Paleozoic Transgressive-Regressive Deposits, in Wilgus, Cheryl K., Hastings, Bruce S., Posamentier, Henry, Wan Wagoner, John, Ross, Charles A., and Kendall, Christopher G. St. C., eds., Sea-Level Changes - An Integrated Approach, SEPM Special Publication No. 42, p. 227-247.

Ruppel, S.C. and Ward, W.B., 2013, Outcrop-based characterization of the Leonardian carbonate platform in west Texas: Implications for sequence-stratigraphic styles in the Lower Permian: AAPG Bulletin, v. 97, no. 2, p. 223-250.

Simms, J., Simms, F., and Suneson, N. H., 1995, The geology of the southwestern Ozark Uplift: an introduction and field-trip guide, Oklahoma Geological Survey Open-File Report 6-95, 27 p.

APPENDIX

THIN SECTIONS

Thin Section Image Labels			
AM	authigenic muscovite	**ML**	mollusc
BF	benthic foraminifer	**PEL**	peloid
BR	brachiopod	**PY**	pyrite
BU	burrow	**Q**	quartz
BY	bryozoan	**ROO**	radial ooid
CC	calcite cement	**SC**	silica cement
CH	chert	**SK**	skeletal fragment
CHL	chalcedony	**SP**	sponge spicule
CR	crinoid	**TOO**	tangential ooid
D	dolomite	**TR**	trilobite
FR	fracture		

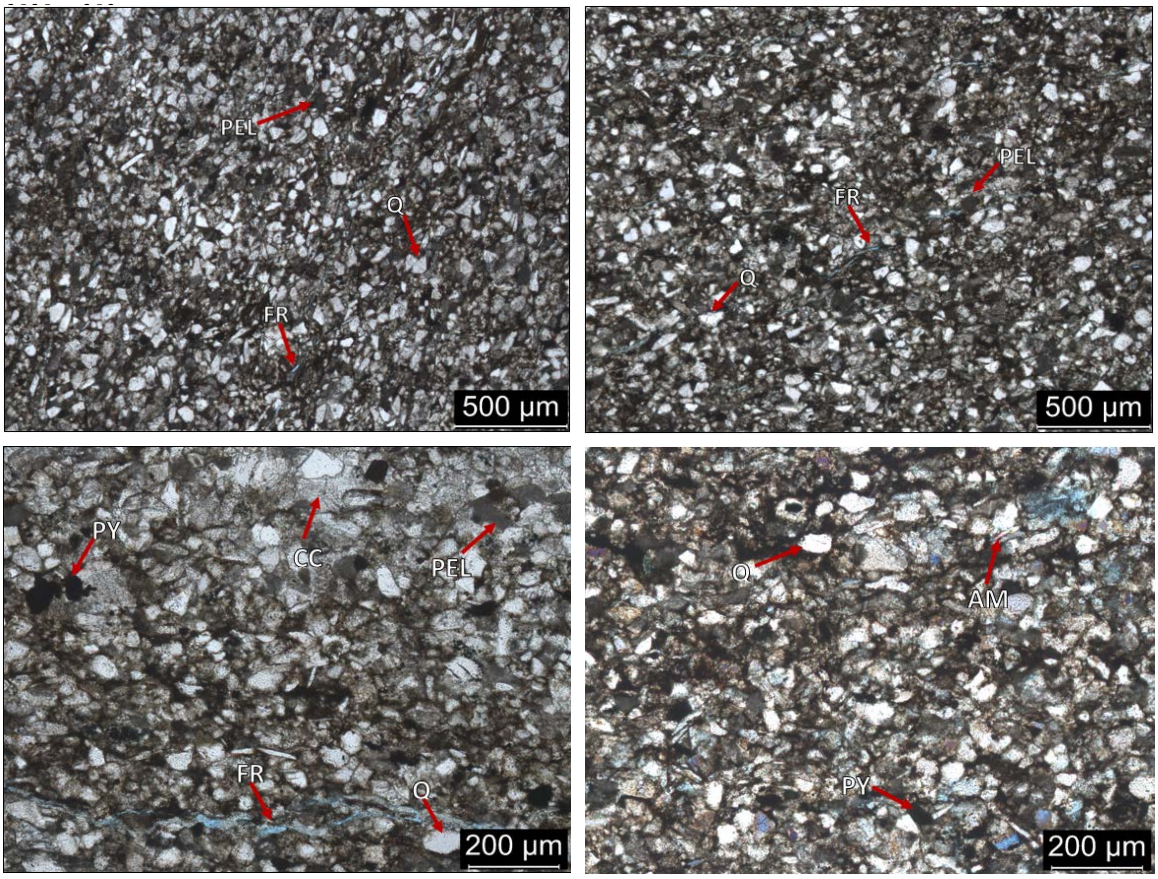

Facies 1 – Clay-Rich Quartz Siltstone – medium silt to fine sand-sized, angular quartz grains within a clay-rich matrix. Contains 45% quartz grains, 40% clay matrix, and 14% calcite, and 1% pyrite (visual estimation). Porosity exists in the form of intergranular, intragranular, vuggy, and fracture pores.

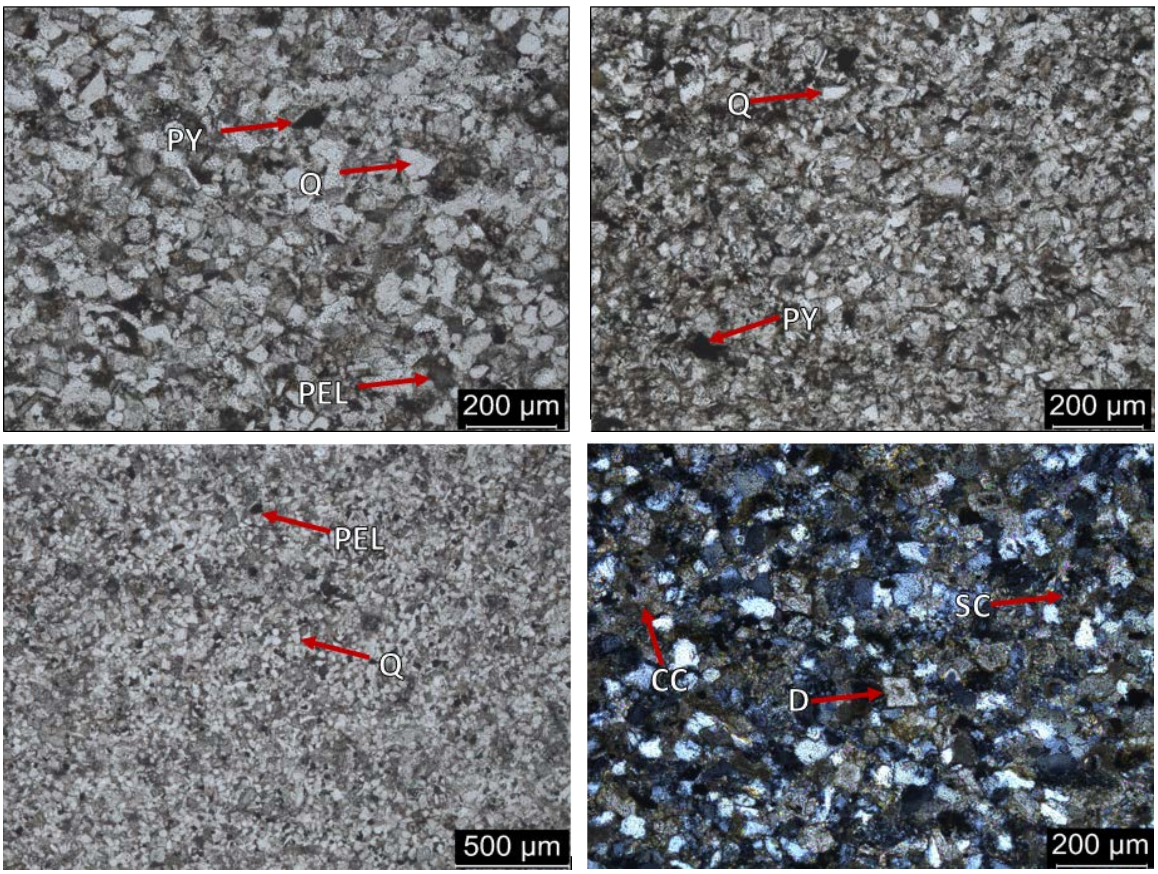

Facies 2 – Calcareous Quartz Siltstone – Medium silt to very fine sand-sized angular quartz grains within a silica and calcite cement matrix. Contains 40% quartz, 35% silica cement, 20% calcite cement, and 5% peloids. Scattered dolomite is observed, but not volumetrically significant.

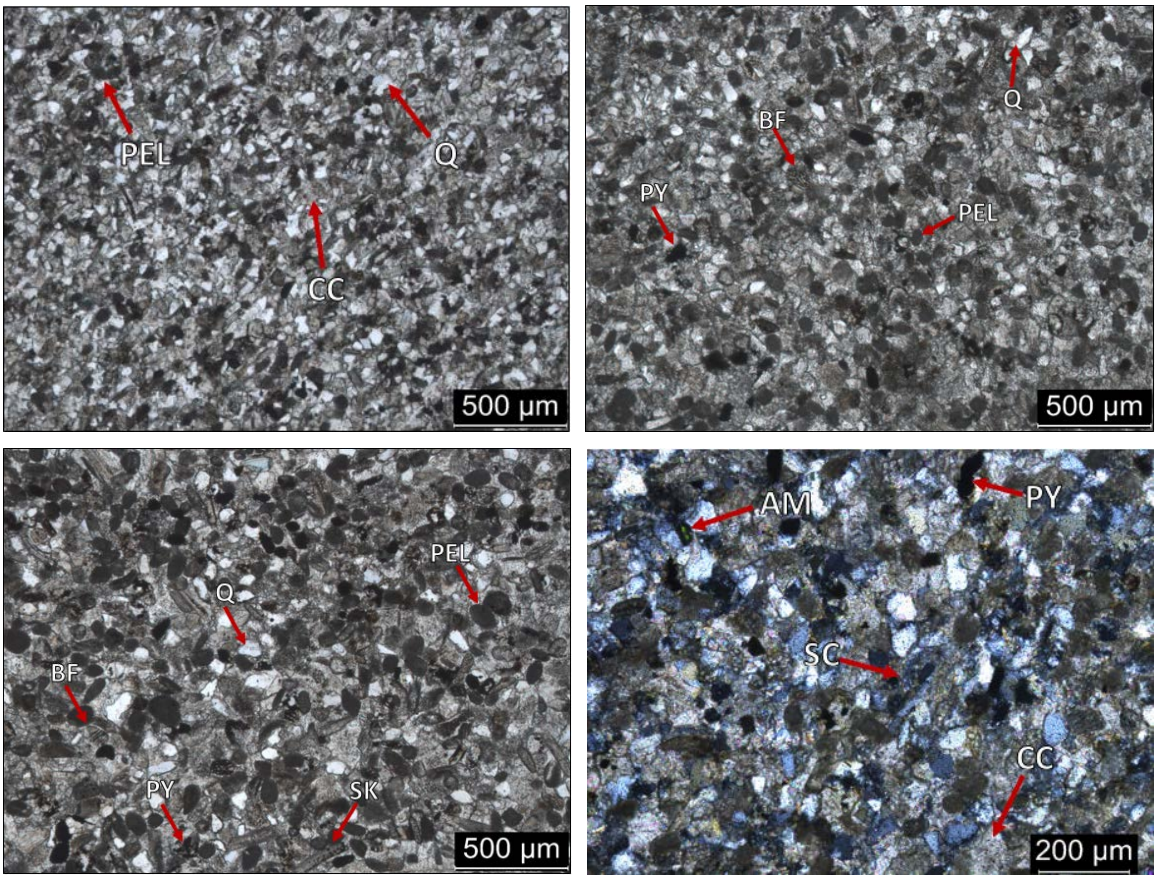

Facies 3 – Calcareous Peloidal Siltstone-Packstone – very fine sand sized quartz and very fine to medium sand sized peloids in a calcite and silica cement matrix. Relative percentages of quartz to peloids vary proportionally, each ranging from 20-50%, with 20% calcite cement, 10% silica cement, 5% skeletal fragments, and scattered authigenic muscovite. Skeletal fragments tend to be made up of brachiopod or crinoid debris.

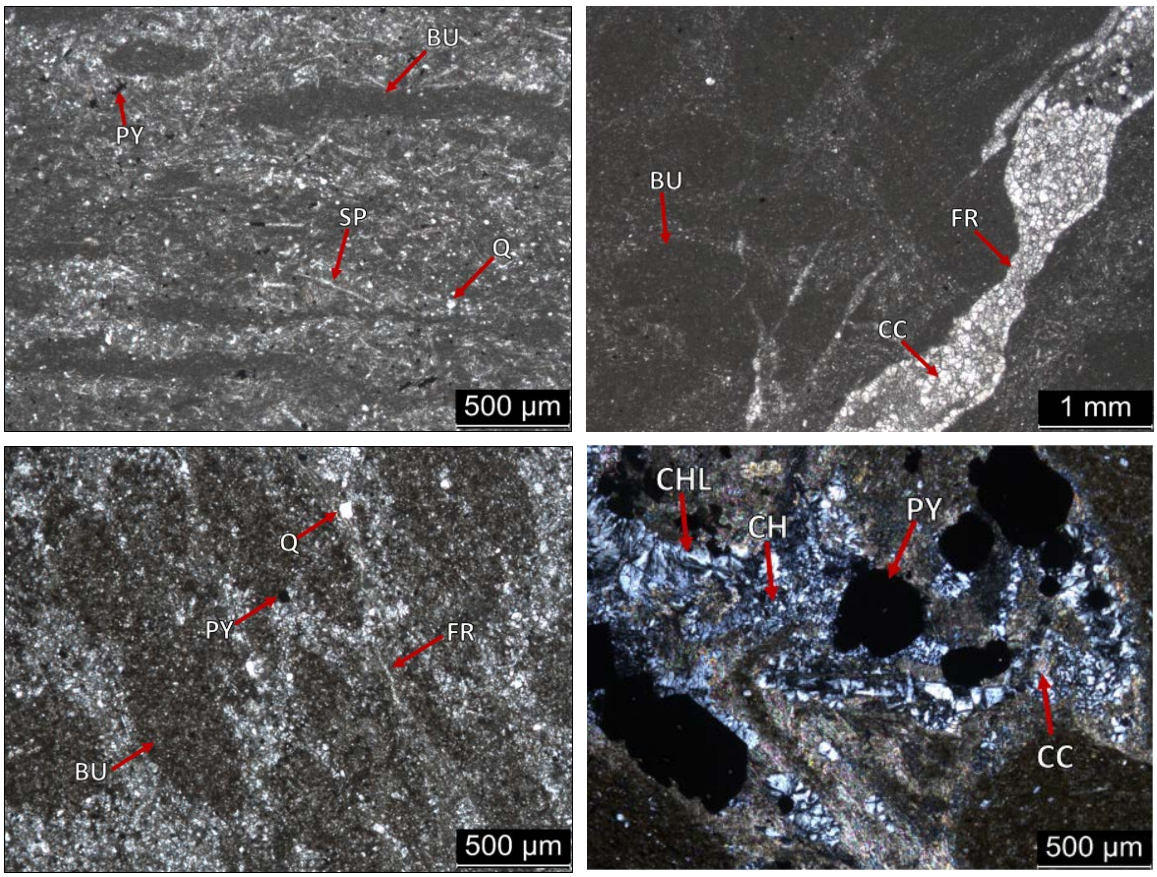

Facies 4 – Burrowed Mudstone-Wackestone – carbonate mud and spicules with occasional bedded cherts. 70% carbonate mud, 20% quartz silt, 5% sponge spicules, 5% silica cement, <1% pyrite. Fractures are most abundant in this facies due to its chert content, and are typically filled with blocky calcite or chalcedony cements.

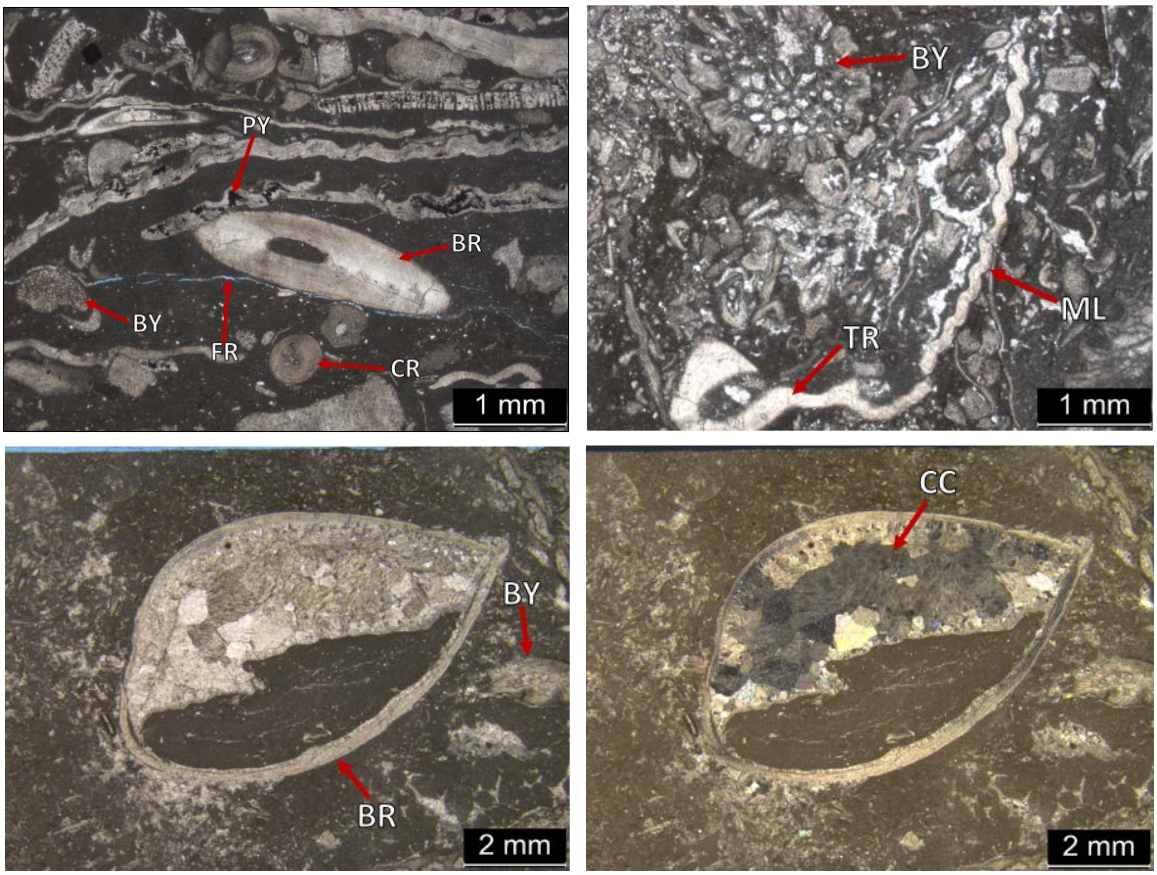

Facies 5 – Skeletal Wackestone – skeletal debris in a carbonate mud matrix. 50% carbonate mud, 40% skeletal grains, 8% calcite cement, 2% quartz silt. Skeletal grains include brachiopods, bryozoans, trilobites, crinoids, and echinoderms. Scattered ooids are observed, but rare. Minimal dissolution-enhanced vuggy porosity exists.

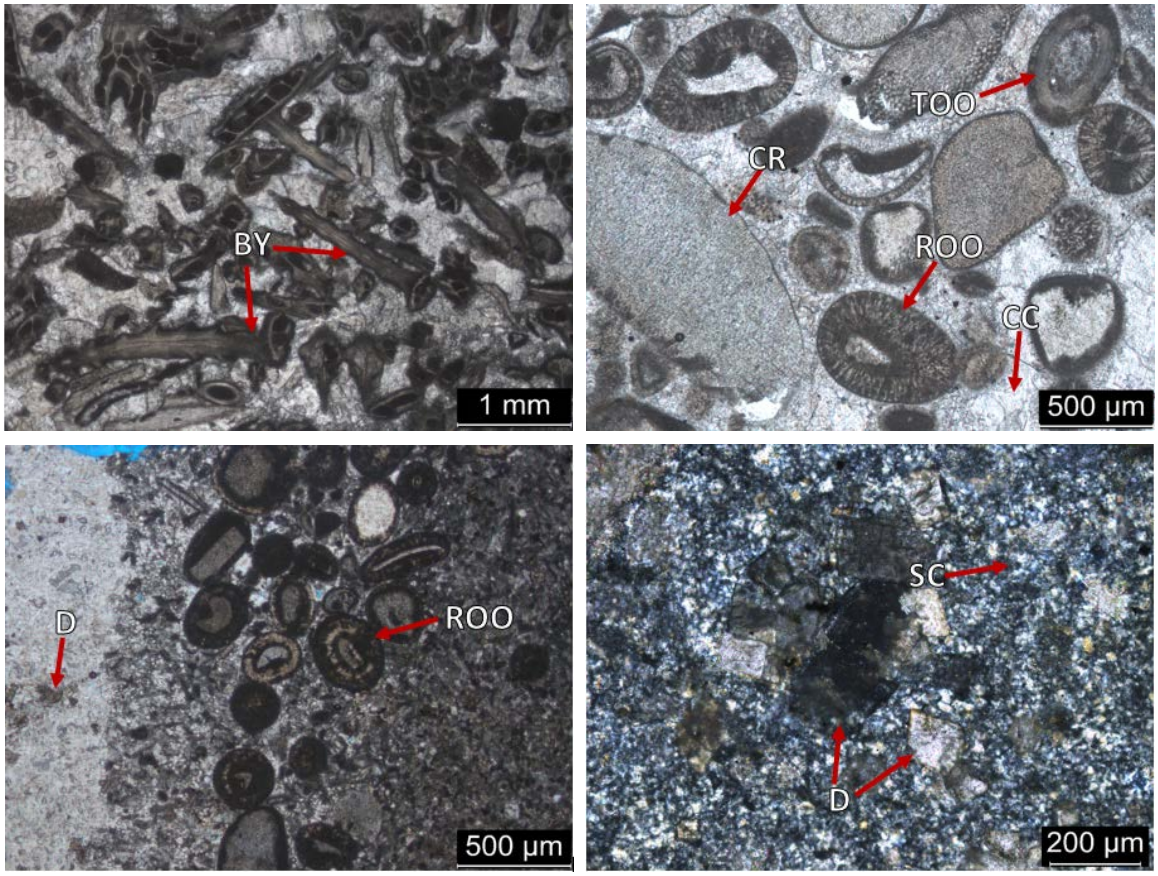

Facies 6 – Skeletal Packstone-Grainstone – skeletal and non-skeletal carbonate grains in a dominantly calcite cement matrix. 40% calcite cement, 35% skeletal grains, 20% ooids, variable silica and dolomite cements. Skeletal content includes brachiopods, bryozoans, crinoids, echinoderms, and benthic foraminifera. Non-skeletal content includes both radial and tangential ooids. Dolomite and silica cements are observable near exposures.

VITA

Scott Andrew Shelley

Candidate for the Degree of

Master of Science

Thesis: OUTCROP-BASED SEQUENCE STRATIGRAPHY AND RESERVOIR CHARACTERIZATION OF AN UPPER MISSISSIPPIAN MIXED CARBONATE-SILICICLASTIC RAMP, MAYES COUNTY, OKLAHOMA

Major Field: Geology

Biographical:

Education:

Completed the requirements for the Master of Science in Geology at Oklahoma State University, Stillwater, Oklahoma in December, 2016.

Completed the requirements for the Bachelor of Science in Geology at Oklahoma State University, Stillwater, Oklahoma in 2014.

Professional Memberships: American Association of Petroleum Geology
Society for Sedimentary Geology
Geological Society of America
Tulsa Geological Society
Oklahoma City Geological Society